}essentials{

Thomas Lauterbach

Radio Astronomy

Small Radio Telescopes: Basics, Technology and Observations

Springer

essentials

Springer essentials

Springer essentials provide up-to-date knowledge in a concentrated form. They aim to deliver the essence of what counts as "state-of-the-art" in the current academic discussion or in practice. With their quick, uncomplicated and comprehensible information, essentials provide:

- an introduction to a current issue within your field of expertise
- an introduction to a new topic of interest
- an insight, in order to be able to join in the discussion on a particular topic

Available in electronic and printed format, the books present expert knowledge from Springer specialist authors in a compact form. They are particularly suitable for use as eBooks on tablet PCs, eBook readers and smartphones. *Springer essentials* form modules of knowledge from the areas economics, social sciences and humanities, technology and natural sciences, as well as from medicine, psychology and health professions, written by renowned Springer-authors across many disciplines.

Thomas Lauterbach

Radio Astronomy

Small Radio Telescopes: Basics, Technology, and Observations

Springer

Thomas Lauterbach
Nürnberg, Germany

ISSN 2731-3107 ISSN 2731-3115 (electronic)
essentials
ISBN 978-3-658-36034-4 ISBN 978-3-658-36035-1 (eBook)
https://doi.org/10.1007/978-3-658-36035-1

This Springer imprint is published by the registered company Springer Fachmedien Wiesbaden GmbH, part of Springer Nature.
The registered company address is: Abraham-Lincoln-Str. 46, 65189 Wiesbaden, Germany

Preface

Radio astronomy is a fascinating field of research – the first image of a black hole, the elucidation of the spiral structure of the Milky Way, the discovery of cosmic background radiation, and the first indirect observation of gravitational waves are just some of the spectacular discoveries made with radio telescopes. For this reason, the Astronomical Society in the European Metropolitan Region Nuremberg decided to establish a special interest group under the leadership of the author in order to set up a radio telescope at Regiomontanus Observatory, Nuremberg, Germany, and thus also to be able to provide the public with insights into this field of astronomy.

Unlike classical astronomy with its view through a telescope, humans have no senses for radio radiation – and this results in the difficulty of understanding the basics of radio astronomy and interpreting its measurements. And this subject does not make it easy for us – in addition to astronomical and physical knowledge, knowledge of radio frequency technology and digital signal processing is also required. These challenges have been successfully met by the special interest group: In monthly seminars, the necessary knowledge was acquired, and a concept for a radio telescope was developed and tested in preliminary experiments. Finally, on April 26, 2019, the radio telescope named after Nobel laureate Arno Penzias could be ceremoniously inaugurated.

The radio astronomy tours, which have been organized repeatedly since then, met with gratifyingly great interest, raised the question of the didactics of radio astronomy as a new challenge. Presentations were developed and exemplary measurements and their explanations were prepared. But the question of some visitors, if it is possible to read all this somewhere, had to be answered negatively, because books about radio astronomy are only available in English and only on university

level. This gave the impulse for this introductory book first published in German and now in an English translation. Many who begin to study radio astronomy, whether at universities, schools, observatories, or even out of personal inclination, will do so with comparatively modest radio telescopes – with dishes with diameters of a few meters. In addition to the fundamentals of radio astronomy, it is the technology and observational capabilities of such "small" radio telescopes that are the focus of this book. Academic radio astronomical research and the technology of the "large" radio telescopes can only be touched upon. Likewise, the detailed explanation of some technical terms had to be omitted. They were nevertheless used, with the "so-called" in front, in order not to withhold them from the reader and to encourage them to delve deeper into the subject matter with the help of the indicated further literature or the Internet.

I would like to express my special thanks to the members of the special interest group and to the students at Nuremberg Institute of Technology (Technische Hochschule Nürnberg Georg Simon Ohm) who worked on projects related to the construction of the radio telescope. Without their enthusiasm, commitment, expertise, and diligence, neither the radio telescope nor this book would have come into being. Furthermore, I would like to thank the board of directors of the Astronomical Society in the European Metropolitan Region Nuremberg for their continuous enthusiastic support as well as the "Zukunftsstiftung der Sparkasse Nürnberg" for their financial support of the radiotelescope project. Last but not least, I would like to thank the publishing house and Dr. Edelhäuser as the editor for many suggestions and the pleasant cooperation.

I hope all readers enjoy their introduction to radio astronomy and gain interesting insights!

Nürnberg, Germany Thomas Lauterbach

What You Can Find in This *essential*

- A brief history of radio astronomy and its discoveries from the first signals of cosmic origin to the imaging of a black hole.
- An overview of electromagnetic waves and the related physical quantities
- An overview of the origin and properties of cosmic radio radiation
- How a radio telescope works and how to evaluate the measurements with it
- Examples of typical observations you can make with a small radio telescope
- An outlook on interferometry, current research topics in radio astronomy, and how to get started in radio astronomy yourself.

Contents

List of Figures

Introduction: What Is Radio Astronomy?

1

1.1 The Development of Astronomy Up to the Nineteenth Century

Astronomy is one of the oldest sciences, because people have always observed the events in the sky, the movement of the sun, the moon and the stars, and tried to understand and interpret them.

The European tradition of astronomy is based on the knowledge of Greek philosophers. Many basic facts such as the spherical shape and size of the earth, the movement of the moon around the earth and that of the earth around the sun were already known to them. Formative for a long time was the astronomical knowledge that *Claudius Ptolemy* had compiled in his work "Almagest" in the second century AD but on the basis of the geocentric system.

The heliocentric view of the world was only reformulated in the sixteenth century by *Nicolaus Copernicus.* But since he held on to circular planetary orbits around the sun, the great success failed to materialize. Only *Johannes Kepler,* who was able to show that the planetary orbits were ellipses, was able to calculate the planetary positions correctly.

Around the same time, the telescope became available as a tool for astronomical observations. *Galileo Galilei's* discoveries have become particularly well known. He was one of the first to use a telescope for celestial observations and from 1609 onwards discovered, among other things, the four large moons of Jupiter, the craters and mountains of the moon and the phases of Venus.

Subsequently, both the performance of telescopes and the mathematical methods of celestial mechanics evolved, especially after *Isaac Newton* formulated the axioms of mechanics.

T. Lauterbach, *Radio Astronomy*, essentials,
https://doi.org/10.1007/978-3-658-36035-1_1

Further observational possibilities did not arise until the advances in science and technology in the nineteenth century when a series of discoveries were made in the field of electricity and magnetism. It was in this context that electromagnetic waves were discovered, the application of which led to radio transmission and eventually to radio astronomy.

1.2 Electromagnetic Waves and Radio Technology

In 1864, *James Clerk Maxwell* presented a theory that encompassed all phenomena of electromagnetism, such as the magnetic effect of electric currents and electromagnetic induction (Poppe 2015). From this theory, it emerged mathematically that electric and magnetic fields can propagate as "electromagnetic waves" (see Chap. 2).

Since their calculated speed corresponded to the speed measured for the light of about 300,000 km/s, the interpretation that light is an electromagnetic wave was obvious. *Heinrich Hertz* succeeded in generating and detecting electromagnetic waves by electrical means in 1888, using dipoles, i.e. two rods with a gap between them. He applied a high voltage across the gap of the transmitting dipole, causing a spark over. At the gap of a second dipole, he could observe that a spark also jumped over there when it was hit by the wave of the first dipole. This confirmed *Maxwell's* theory.

Soon after, *Guglielmo Marconi* began experimenting with similar transmitters and receivers in Italy and England. He was able to increase the range of transmission to several kilometers. This new technology was called "wireless" telegraphy or radio, from the Latin radius, if the focus is on the beam emitted by the transmitter.

The further development of radio technology concentrated on the long wave range with wavelengths of several kilometres, as overseas radio telegraphy was possible there. In the USA, non-commercial amateur radio stations had also established themselves. These were no longer allowed to use long waves after World War I, so they began experimenting with shorter wavelengths. Finally, in 1921, they succeeded in transmitting a signal at a wavelength of 230 m across the Atlantic, although the most powerful amateur station "1BCG" in Greenwich, Ct, USA had less than one hundredth of the transmitting power of a commercial long wave station.

After this success and due to the availability of new electronic components such as electron tubes and crystal oscillators, radio technology became established in

the short wave range down to about 10 m wavelength (30 MHz). Since the waves in short wave transmission are reflected by conductive layers of the upper atmosphere (ionosphere) at an altitude of up to 400 km, antennas were used for this purpose which could focus the waves obliquely upwards or also receive them from obliquely above.

By the end of the 1920s, short wave technology had advanced to the point where it could be used not only for radiotelegraphy but also for the transmission of overseas telephone calls and broadcasts.

1.3 Karl Jansky and Grote Reber: The Beginning of Radio Astronomy

With the short wave telephone transmission, however, interferences occurred again and again by strong noise and crackling and hissing sounds. At the US-American Bell telephone company, research was therefore carried out into the causes of this interference. For this purpose, *Karl Guthe Jansky* built a sensitive receiver with which he could record the noise level, as well as a directional antenna which rotated once in a circle in 20 minutes (Fig. 1.1). The measurements were made at a wavelength of 14.6 m (20.5 MHz). It quickly became apparent that most of the interference was caused by thunderstorms. However, *Jansky* also observed a hissing noise that recurred regularly and came in from different directions over the course of a day. By taking repeated measurements over a year, he concluded that this signal must have an extraterrestrial cause, since the times at which it occurred and the direction from which it came coincided with the movement of a region in the constellation Sagittarius in the sky. *Jansky* published this conclusion in 1933 (Nesti 2019). He had thus founded the new field of radio astronomy, even though he did not pursue it himself.

Through *Jansky's* publications, which the "New York Times" had even reported on its front page, *Grote Reber,* a radio amateur and amateur astronomer, became aware of the subject. In 1937, he was the first to build a radio telescope, i.e., a receiving facility built specifically to receive signals from the cosmos. As an antenna, he chose a type that is still characteristic of radio astronomy today: a parabolic reflector about 9 m in diameter with the receiver at the focal point (Fig. 1.2). *Reber*

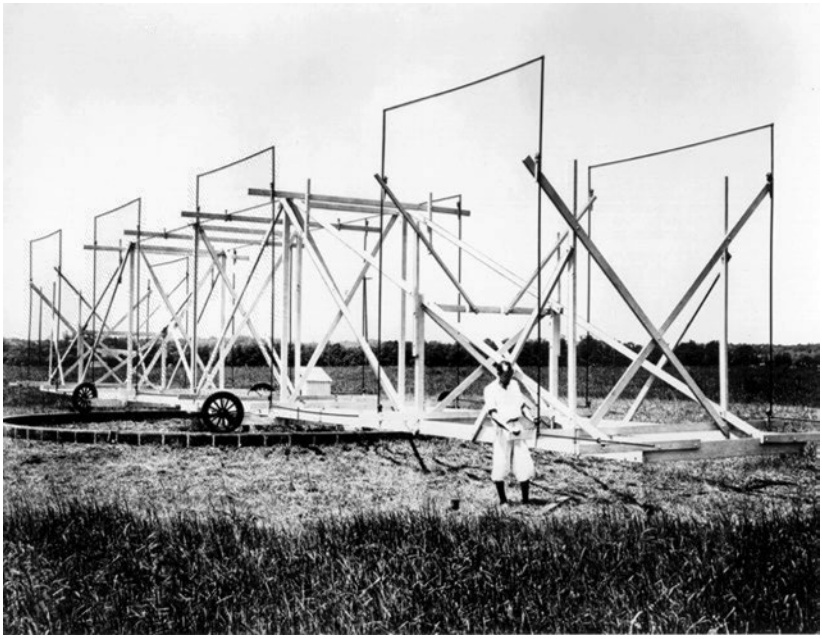

Fig. 1.1 *Karl G. Jansky* and his rotatable directional antenna. (Credit: NRAO/AUI/NSF)

used this to scan the sky and in 1944 published a radio map at a wavelength of 1.9 m (160 MHz).

1.4 The Further Development of Radio Astronomy

Due to the rapid development of radio and radar technology during the Second World War, radio astronomy became a rapidly growing branch of science from 1945 onwards, making important contributions to the understanding of the Universe and continuing to do so to this day (Kraus 1964; Mezger 1984). Following the strong emission from the Sun, which had already attracted attention due to interference to radar during the war, a number of radio sources were identified in the Milky Way and beyond. Since 1948, the terms “radio astronomy” and “radio telescope” became established (Algeo and Algeo 1993, pp. 124, 136).

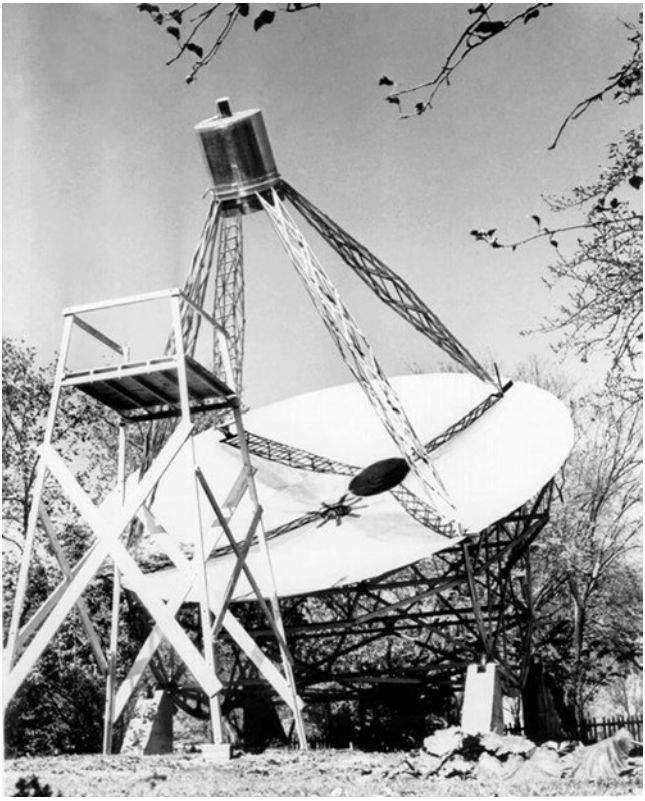

Fig. 1.2 *Grote Reber's* 31-foot radio telescope in Wheaton, Illinois, USA, about 20 km west of Chicago. (Credit: NRAO/AUI/NSF)

A milestone was the first successful measurement of 21-cm radiation of neutral hydrogen from gas clouds in the Milky Way by *Harold Ewen* and *Edward Purcell* at Harvard University in 1951 (Fig. 1.3) and by a Dutch research group (Stephan 1999). This radiation had already been predicted in 1945 by *Hendrik van de Hulst*. It was now possible to observe not only hot gases emitting visible light, but also very thin and cool hydrogen regions in the Milky Way arms, in which there is only about 1 atom per cm^3. With the help of the Doppler shift of this radiation, the spiral structure of the Milky Way and the mutual motion of the Milky Way arms could be detected (see Sect. 4.3). In the same year, the radio source "Cygnus A" was identified as a galaxy about 800 million light years away.

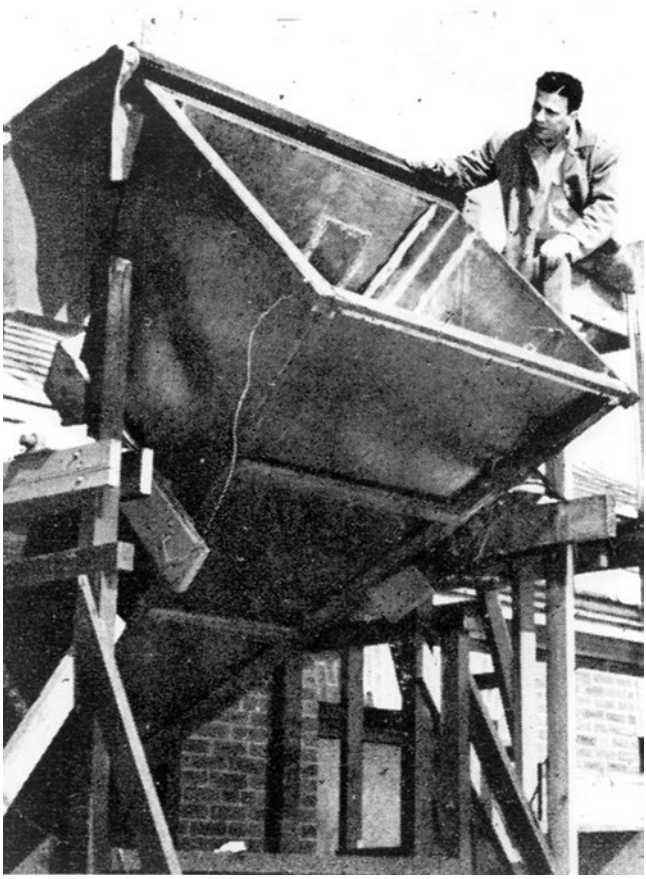

Fig. 1.3 *Harold Ewen* inspects the Horn antenna with which he was able to measure the 21-cm radiation of neutral hydrogen for the first time in 1951. (Credit: NRAO/AUI/NSF)

Further discoveries of various galactic and extragalactic radio sources followed as ever larger fixed and partially or fully directional movable radio telescopes were built, many with parabolic reflectors of 80 to 100 m in diameter (e.g. Jodrell Bank, Stockert, Effelsberg, Green Bank, Parkes), and even up to 600 m in diameter for stationary facilities (Arecibo, FAST, RATAN-600). The reception range was also extended to ever higher frequencies (e.g. ALMA), but also the long wave end of the radio window (LOFAR).

With the Arecibo radio telescope, radar measurements of the distances to the neighbouring planets, in particular Venus, were also carried out. This allowed the so-called astronomical unit, the mean distance of the Earth from the Sun, to be determined precisely – and thus also the distances of all the other planets from the Sun, since Kepler's third Law results in a direct relationship between the distance and orbital period of a planet. Likewise, structures on the Moon and Venus could be detected with radar. The temperatures of the planetary surfaces were also determined by their radio radiation.

In 1963, the previously known point-like radio source 3 C 273, which had been assumed to be a star, was identified as a galaxy 2.4 billion light-years from Earth. Such objects are called "quasi-stellar radio sources", or "quasars" for short.

In 1964, while attempting to calibrate an antenna of the Bell Telephone Company for radio astronomical observations, which was no longer needed for satellite transmission, *Arno Penzias* and *Robert Wilson* (Fig. 1.4) encountered a constant and uniformly incident noise from all directions, which corresponds to temperature radiation of 2.7 K (Bahr et al. 2014). This so-called cosmic background radiation has been identified as the radiation that arose when, after the Big Bang, the expansion of the universe caused the temperature to drop enough for atoms to form. As a result of further expansion since then, the wavelength of this originally ultraviolet radiation increased to such an extent that it is now in the microwave range.

Jocelyn Bell and *Antony Hewish* discovered a rapidly pulsating radio source in 1967, which was called a "pulsar" by analogy with quasars. This pulsating radio radiation was found to be emitted by a rapidly rotating neutron star, formed after the explosion of a massive star. By observing the orbital change of a double pulsar, *Russell Hulse* and *Joseph Taylor* were able to indirectly detect the emission of gravitational waves by radio astronomy as early as 1978, which can only be observed directly with the LIGO detectors since 2016.

Recently, radio astronomy made headlines with the first direct imaging of a black hole by the Event Horizon Telescope Project (Bouman 2020). For this purpose, seven radio telescopes worldwide were operated together as a "very-long-baseline interferometer" (see Sect. 5.1) at a wavelength of 1.3 mm (230 GHz). The resolving power thus corresponds to that of a radio telescope with the diameter of the Earth. At this wavelength, the gas and dust clouds in the galaxies absorb very little, so that the central region can be observed. However, the turbulent Earth's atmosphere and water vapor interfere with the signals. Measurements are therefore only possible with radio telescopes on high mountains during clear nights. From

Fig. 1.4 *Robert Wilson* and *Arno Penzias* in front of the Horn antenna in Holmdel, N.J., USA, with which they discovered the cosmic background radiation in 1964. (Reused with permission of Nokia Corporation and AT&T Archives)

measurements over four nights in April 2017, an image showing the environment around the black hole could be calculated from a data set of about 5000 terabytes (Fig. 1.5). The bright radiation comes from the so-called accretion disk, in which hot material orbits around the black hole. The dark region in the middle of it is the "shadow" around the event horizon. No electromagnetic waves can escape from this region because of the gravitational pull of the black hole. It is about the size of our solar system. In 2022 the Event Horizon Telescope Collaboration published a similar view of the black hole in the center of the Milky Way.

Fig. 1.5 The image of the region around the black hole in the centre of the galaxy M 87 calculated from radio astronomical measurements. (Credit: EHT Collaboration)

1.5 The Nuremberg "Arno Penzias Radio Telescope"

As an example of a small radio telescope, which serves mainly educational and demonstration purposes, the Arno Penzias Radio Telescope, inaugurated at Regiomontanus Observatory in Nuremberg, Germany in 2019, is presented here. The details of the technology of a radio telescope are explained in Chap. 3, measurements with it are presented in Chap. 4.

During planning, the question arose which radio astronomical observations could be demonstrated at a public observatory with a broad target audience. The 21-cm hydrogen radiation seemed to be the most suitable since it can be detected with a moderate amount of equipment, and it provides interesting insights into the structure of the Milky Way and leads to current research questions such as "dark matter". A radio telescope with a 3-m parabolic antenna is well suited for this purpose. The planning was therefore based on the concept of the "Small Radio Telescope" of the MIT Haystack Observatory, which uses a mesh dish with an antenna rotor for azimuth and elevation. This is mounted on a tiltable tower, and a small office container serves as the base for it and as the service building, in which the receiving electronics are housed (Fig. 1.6). The complete signal processing as well as, the evaluation and display of the received signals are carried out digitally on a PC, as is the operation of the antenna rotor and the configuration of the measurements. This can also be done remotely via an Internet connection, so that

Fig. 1.6 The "Arno Penzias Radio Telescope" set up by the Astronomical Society in the European Metropolitan Region Nuremberg at Regiomontanus Observatory, Nuremberg, Germany. The small 1.5 m antenna in the front right serves as test equipment. (Photo: Thomas Lauterbach)

demonstrations are possible not only in the lecture hall of the observatory but also, for example, in the Nicolaus Copernicus Planetarium of the city of Nuremberg and schools and universities.

Summary

Until the twentieth century, astronomy relied on optical observations; it was not until the use of electromagnetic waves by radio technology that observations could be extended to other frequency ranges: Radio astronomy led to the discovery of numerous cosmic radio sources, the 21-cm radiation of hydrogen, the cosmic background radiation, quasars and pulsars. Modern interferometric methods and data processing allow spectacular images, e.g. that of a black hole.

What Are Electromagnetic Waves? 2

2.1 Basic Properties of Electromagnetic Waves

In electromagnetic waves, electric and magnetic fields propagate together. Figure 2.1 shows a snapshot of a plane wave. The wavelength is the distance between two points of the wave with the same properties, e.g. between two successive wave crests. The frequency indicates how often, for example, a wave crest passes a fixed location as the wave propagates. The unit of frequency is named after *Heinrich Hertz*: at a frequency of 1 Hertz (Hz), one wave crest is observed per second. The time interval between the wave crests is the period $T = 1/f$. Since the wave moves on by one wavelength during the period, the relation between the propagation speed c (speed of light, in vacuum $3 \cdot 10^8$ m/s), the wavelength λ and the frequency f is given by:

$$c = \frac{\lambda}{T} = \lambda \cdot f. \tag{2.1}$$

Example

The frequency of 1420.4 MHz frequently observed in radio astronomy corresponds to a wavelength of 21.106 cm.

If in a wave, as shown in Fig. 2.1, the field strengths each oscillate in a fixed plane, the wave is said to be linearly polarized. If the fields rotate around the axis in the direction of propagation, the wave is circularly or elliptically polarized. ◄

T. Lauterbach, *Radio Astronomy*, essentials,
https://doi.org/10.1007/978-3-658-36035-1_2

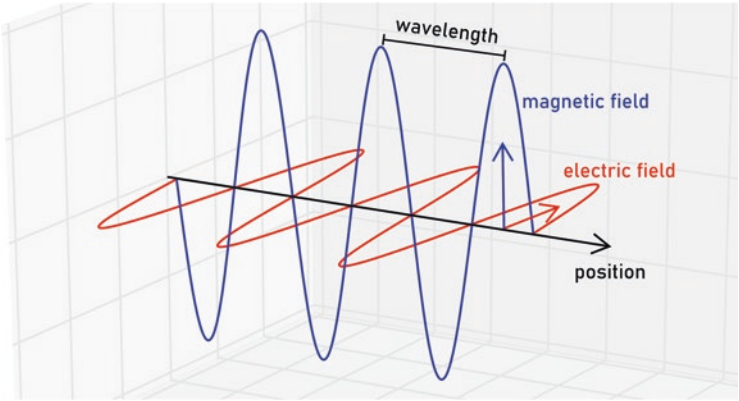

Fig. 2.1 Example of the spatial course of the fields for a harmonic linearly polarized plane electromagnetic wave (snapshot)

2.2 The Spectrum of Electromagnetic Waves

The spectrum that can be used today, i.e. the frequency or wavelength range of electromagnetic waves, extends from a few Hertz to over 10^{18} Hz. Figure 2.2 shows the different frequency ranges, starting with radio waves, which are used for a variety of applications such as television, mobile phones and radar. The frequencies for these range from a few kilohertz (10^3 Hz) to 300 Gigahertz (10^9 Hz). Body scanners at airports, for example, operate in the THz (10^{12} Hz) range. Humans have no sensory organs for any of these electromagnetic waves. We can only feel the thermal radiation at the border to visible light on our skin and perceive the visible light (around $6 \bullet 10^{14}$ Hz) with our eyes. In the ultraviolet, X-ray and gamma radiation range, the energy of the radiation is so high that atoms and molecules can be broken down into their constituent parts (ionizing radiation). This can lead to the formation of chemically active substances that can cause cancer, for example.

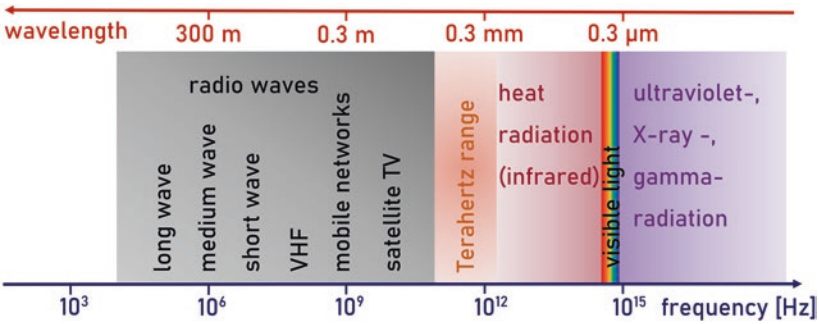

Fig. 2.2 The electromagnetic spectrum

This is because the energy of electromagnetic waves is not continuous but quantized: a quantum (photon) carries the energy $E = h \cdot f$, at the frequency f and can only be emitted or absorbed as a whole (h denotes Planck's constant, $h = 6.63 \cdot 10^{-34}$ J · s). Quantum energies are often expressed in units of "electron volts" (eV). 1 eV is the energy gained by an electron when passing through a voltage of 1 V ($1.6 \cdot 10^{-19}$ J).

Example

1 eV is met at $2.4 \cdot 10^{14}$ Hz in the near-infrared range, about 3 eV at violet light, X-ray and gamma quanta have energies in the keV and MeV range. In the radio wave range, quantum energies are in the µeV range, e.g. 5.8 µeV at 1.4 GHz. ◄

2.3 Which Electromagnetic Waves Can Be Used for Radio Astronomy?

The electromagnetic waves do not need any carrier substance, therefore they can propagate through the vacuum and the almost equally empty universe. We can thus obtain information about cosmic objects by observing the electromagnetic waves generated by them.

However, the Earth is surrounded by its atmosphere, and therefore the entire spectrum of electromagnetic waves cannot be used for astronomical observations from the Earth's surface. Rather, there are only two "windows" into space: the "optical window" in the range of visible light and the "radio window"

(Fig. 2.3). In the frequency range below about 30 MHz, the ionosphere, which consists of electrically charged layers of air at altitudes of 60 to 400 km, is impermeable to electromagnetic waves. At frequencies between about 300 GHz and the infrared range, numerous molecules such as water, carbon dioxide and methane absorb the waves. This attenuating influence of the Earth's atmosphere is already noticeable at the short wave end of the radio window. Radio telescopes for wavelengths in the millimeter range are therefore operated on high mountains. Only in the visible range is the atmosphere transparent again under clear skies and can be used for astronomical observations. In contrast to the optical range, because of the longer wavelength, the scattering of the waves by the atmosphere in large parts of the radio window is so low that observations can also be made during the day.

Another problem is the heavy use of the radio range by radio, radar etc. For radio astronomy, therefore, some frequency ranges are reserved in which it is not permitted to transmit, e.g. the range 1400–1427 MHz, in which the radiation of neutral hydrogen can be observed. In other frequency ranges, interference-free reception is often not possible. Radio telescopes are therefore often built-in remote locations where there is little radio traffic. However, radio transmissions from satellites can also impair reception there. After all, even the signal from a mobile phone on the Moon would have intensity on Earth comparable to that of cosmic radio sources. The ideal location for a radio telescope is therefore considered to be on the far side of the Moon, which is always turned away from the Earth.

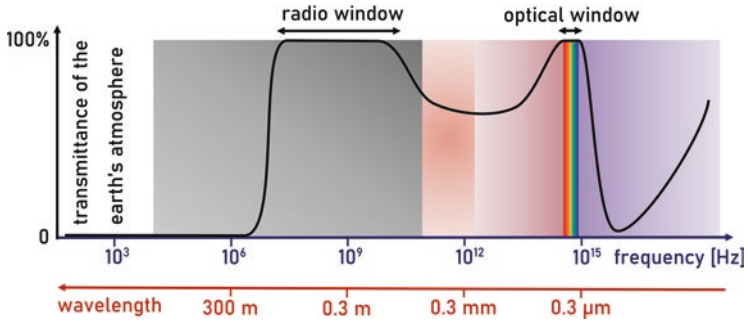

Fig. 2.3 The transmittance of the Earth's atmosphere to electromagnetic waves (schematic)

2.4 Physical Quantities of Electromagnetic Waves

To characterize a continuous electromagnetic wave as shown in Fig. 2.1, it is sufficient to specify the wavelength or frequency, the polarization direction and the maximum value of the electric or magnetic field strength. The two field strengths are linked via the so-called characteristic impedance of the vacuum Z_0 = 377 Ω: $E_{max} = Z_0 \cdot H_{max}$. Usually, the intensity S of the wave is specified, which is the power that is transported through a cross-sectional area averaged over a suitable time interval τ. The term power flux density is also used for this quantity.

Physical Quantities for Characterizing the Strength of Electromagnetic Radiation

The correlation of the intensity S with the electric or magnetic field strength is quadratic, i.e.

$$S = \frac{1}{Z_0 \tau} \int_0^{\tau} E(t)^2 \, dt = \frac{Z_0}{\tau} \int_0^{\tau} H(t)^2 \, dt \tag{2.2}$$

One can easily calculate the intensity of a source if it has a total (mean) radiated power P_S in all directions. The power is then distributed over the spherical surface $A = 4\pi r^2$ at a distance r and hence:

$$S = \frac{P_S}{4\pi r^2} \tag{2.3}$$

The unit of intensity is watts/meter^2. Since the radio radiation of most cosmic sources corresponds to noise, its intensity is distributed over a larger frequency range. Therefore the intensity is related to a frequency interval Δf and then referred to as the spectral intensity S_f, measured in Watt/(Meter^2 Hertz). The intensity measured at frequency f then depends on the bandwidth B of the receiver and is given by:

$$S(f) = \int_{f-\frac{B}{2}}^{f+\frac{B}{2}} S_f(\upsilon) d\upsilon. \tag{2.4}$$

Often the bandwidth B of the receiver is much smaller than the frequency scale on which the spectral intensity changes significantly, then Eq. 2.4 simplifies to:

$$S(f) \approx S_f(f) \cdot B \tag{2.5}$$

Equation 2.3 implies that the intensities of cosmic sources are very small because of the large distance, since doubling the distance to a source results in only a quarter of the intensity, and so on. S_f is therefore given in units of "Jansky" (Jy), 1 Jy = 10^{-26} W/(m^{2}Hz). Examples of the strength of cosmic sources are given in Sect. 2.5.

Questions

Calculate the spectral intensity on Earth produced by a mobile phone (GSM) on the Moon (1 W transmit power, 170 kHz bandwidth). Average distance Earth-Moon: 384,000 km.

Result: 318 Jy.

2.5 Cosmic Radio Sources

The electromagnetic radiation of cosmic objects is produced by different physical processes. A distinction is made between mechanisms that produce continuous radiation over a wider frequency range and those that result in radiation only in a narrow frequency band (line spectrum).

2.5.1 Thermal Radiation

A process with a continuous spectrum known from everyday life is thermal radiation, as can be observed in a light bulb or a hot hotplate. It is described by Planck's radiation law, and the associated spectral intensity is shown in Fig. 2.4. For the calculation, it was assumed that this is uniformly incident (isotropic) from all directions. The Planck curve has a maximum which depends on the temperature of the radiating surface. At 300 K this is in the infrared region, and at 6000 K, the approximate temperature of the solar surface is in the visible region. In the radio window, the spectral intensity increases with the square of the frequency for thermal radiation (Rayleigh-Jeans radiation law). Therefore, for sources whose intensity has been measured at several frequencies and which exhibit this behavior, it can be concluded that their radiation is produced by thermal processes, such as hot surfaces or gases. Examples of such sources are the Moon and the planets, whose surfaces are heated by solar radiation and possibly internal processes (Fig. 2.5). In

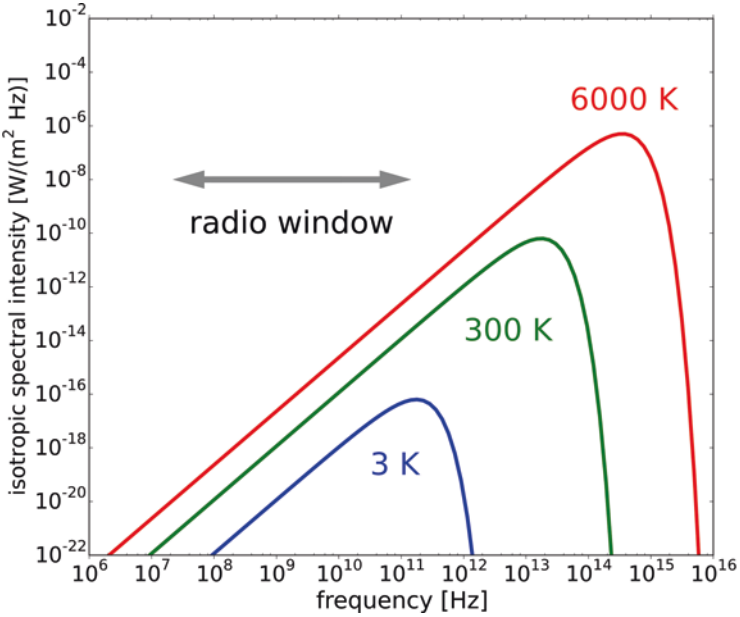

Fig. 2.4 Spectral intensity of thermal radiators at different temperatures according to Planck's radiation law

the case of thermal emission by ionized gases (plasmas), such as in the Orion nebula (Fig. 2.5), a cloud of hydrogen gas ionized by the radiation of a star within it, the course of the spectral intensity follows Rayleigh-Jeans' law only at low frequencies, while it is frequency-independent at higher frequencies.

The laws of thermal radiation allow characterizing astronomical radio sources by their so-called radiation temperature. Even if the radiation is not thermally generated, its spectral intensity can be described, at least in a small frequency interval around the observation frequency f, by the temperature T that a thermal source would have to have to produce the same spectral intensity (Burke et al. 2019, pp. 71 ff.). The relation for isotropic radiation is given by ($k_B = 1.38 \cdot 10^{-23}$ J/K is the so-called Boltzmann constant):

$$S_f = \frac{8\pi k_B T}{c^2} f^2 \tag{2.6}$$

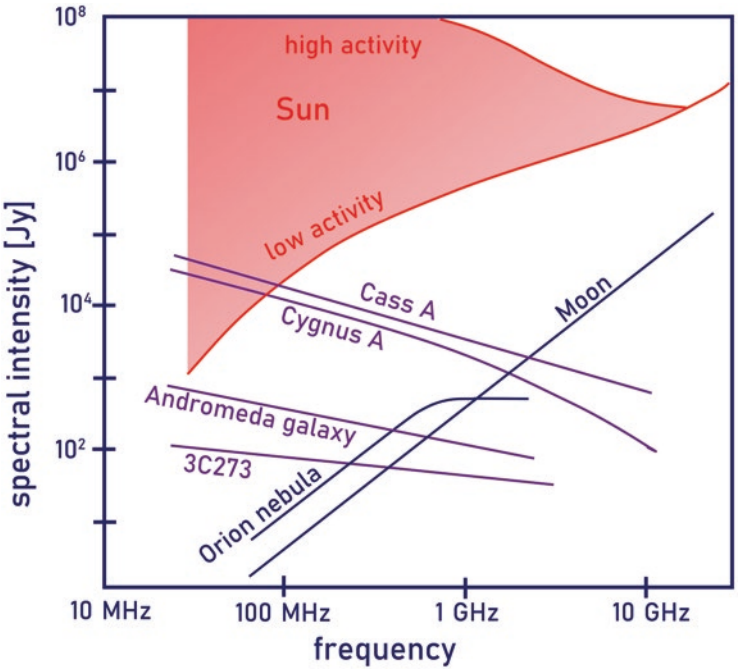

Fig. 2.5 Overview of the spectral intensity of some strong cosmic radio sources in the VHF and microwave range. Red: radio radiation from the sun, dark blue: thermal sources, violet: synchrotron radiation

In contrast to the visible radiation, which corresponds to a Planck radiation of about 5770 K, the radio radiation of the Sun is predominantly of non-thermal origin at frequencies below 10 GHz. In particular, in the frequency range up to a few Gigahertz, the radiation comes predominantly from the corona, a zone of hot ionized gas (plasma) surrounding the visible solar disk. The size and strength of the corona depend on the fluctuating solar activity. The 11-year sunspot cycle has a particularly strong effect: In phases of high solar activity with numerous visible sunspots, the radio emission can be up to 10,000 times stronger than during the activity minimum. Furthermore, short-lived solar radiation outbursts are occasionally observed, during which the solar radio radiation also increases strongly.

2.5.2 Non-thermal Continuous Radiation

However, there are also cosmic radio sources where the spectral intensity does not increase with frequency, but is almost constant or even decreases. These include the radio galaxies Cygnus A and 3C 273 and supernova remnants such as Cassiopeia A. The radio radiation is produced by electrons being accelerated to nearly the speed of light by the black hole at the center of a galaxy or by the stellar explosion. When these relativistic electrons enter a magnetic field, they are deflected by the so-called Lorentz force. In this process, electromagnetic waves are emitted by the so-called synchrotron radiation. This name comes from a type of particle accelerator used in basic research where this radiation also occurs. Scattering by other electrically charged particles can also lead to radiation emission.

The spectral intensity of the radio galaxy 3C 273 is only slightly lower than that of the Andromeda galaxy. However, 3C 273 is about 1000 times farther away from Earth (2.5 billion light-years). According to Eq. 2.3, this means that the power of this radiation source is a million times stronger than that of a "normal" galaxy like Andromeda. Even more dramatic is the difference between Cassiopeia A (remnant of a supernova in 1680, distance 11,000 light-years), and the radio galaxy Cygnus A (distance 760 million light-years), both of which have comparable intensities. Here the distance ratio is just under 70,000 and thus the power ratio is almost 5 billion. This shows what enormous processes take place in a radio galaxy compared to the explosion of a star.

The exact processes in strongly radiating radio galaxies are the subject of current research (Burke et al. 2019, Chapter 16). From the region around a supermassive black hole in the centre of the galaxy, two strongly focused jets of matter emerge in opposite directions at relativistic velocities. These jets hit the intergalactic medium outside the galaxy, where they emit their energy over a large area, which is also where the radio radiation originates. The intensity of the radiation striking the Earth depends strongly on the orientation of the two radiation regions to the direction of observation. Overall, however, only about 1% of all galaxies show such strong radio radiation.

2.5.3 The 21-cm Radiation of Neutral Hydrogen

Line sources represent a completely different type of radiation source. They emit or absorb electromagnetic waves only at very specific frequencies. This is associated with a transition between states of the electrons in the atomic shell. The

quantum energy of the emitted or absorbed radiation then corresponds to the energy difference of the states. This will be explained in more detail using the example of the 21-cm radiation of atomic hydrogen.

A hydrogen atom consists of a proton, which is the positively charged atomic nucleus, and a negatively charged electron, which is located in a region around it because it is attracted by the proton due to its opposite charge. The possible states that the electron can be in are quantum mechanically described by four quantum numbers, the principal quantum number *n,* the angular momentum quantum number ℓ, the magnetic quantum number *m* and the spin quantum number *s.* In each state, the electron has defined energy, which is usually given as the binding energy, i.e., the energy that must be applied to release the electron from the corresponding state and thus separate it from the proton (ionization). The binding energy of the electron in the ground state of the hydrogen atom with $n = 1$ is 13.6 eV. The quantum energies for the transitions between the states with different principal quantum numbers are also several electron volts and the associated radiation is thus in the ultraviolet and visible spectral range (e.g. the spectral lines of the so-called Lyman and Balmer series). However, the binding energy of the ground state also depends on the spin quantum number. Since, in addition to the electron, the proton also has a spin, the two states with parallel and antiparallel spin alignment of the proton and electron differ by 5.88 μeV, with the parallel spin state having less binding energy. This splitting is called the "hyperfine structure" of the ground state (Fig. 2.6). As the electron transitions from the less strongly bound (parallel spins) to the more strongly bound state (antiparallel spins), a quantum of radiation with a frequency of 1420.405 MHz is released. Since such radiation appears in a spectrum as a narrow "peak", it is called a spectral line (Fig. 2.7).

Whether a hydrogen cloud in the interstellar medium absorbs or emits 21-cm radiation depends on the temperature to which the gas has been heated by cosmic rays. If this is so high that there are more atoms in the parallel spin state, they gradually transition to the antiparallel state with a half-life (time for half the atoms to complete the transition) of about 11 million years, emitting one quantum of radiation at a time. Although the interstellar hydrogen clouds are very thin (about 1 atom/cm^3), such transitions occur constantly, so that continuous radiation can be observed.

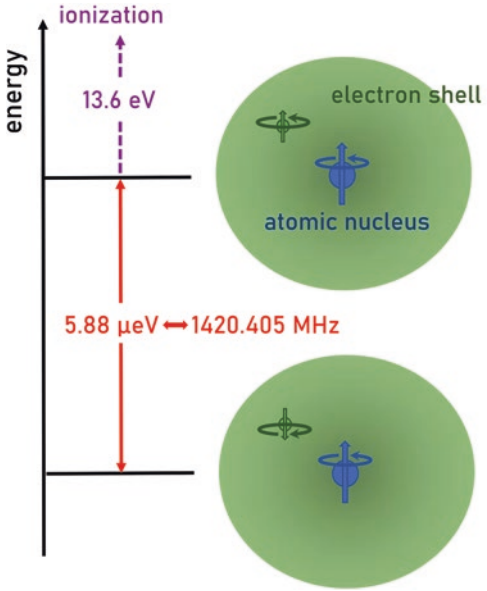

Fig. 2.6 The hyperfine structure splitting of the ground state in the hydrogen atom due to the interaction of the electron shell with the spin of the atomic nucleus. During the "spin flip", the transition from the state with parallel spins to the energetically lower state with antiparallel spins, the energy of 5.88 μeV is released

Already at the first measurement of the 21-cm radiation from gas clouds in the Milky Way arms (see Chap. 1) *Ewen* found out that the radiation is not exactly at the frequency 1420.405 MHz. It is rather shifted against it by some 100 kHz. Furthermore, not a sharp spectral line is observed, but a maximum of several tens of kilohertz wide. Both effects can be explained by the Doppler effect (Fig. 2.7). If a source of electromagnetic radiation and a receiver move towards each other, their frequency appears to shift to higher values. If the distance increases, a lower frequency is observed. The fact that the atoms within a gas cloud move in different directions causes a broadening of the spectral line (Doppler broadening). If, in

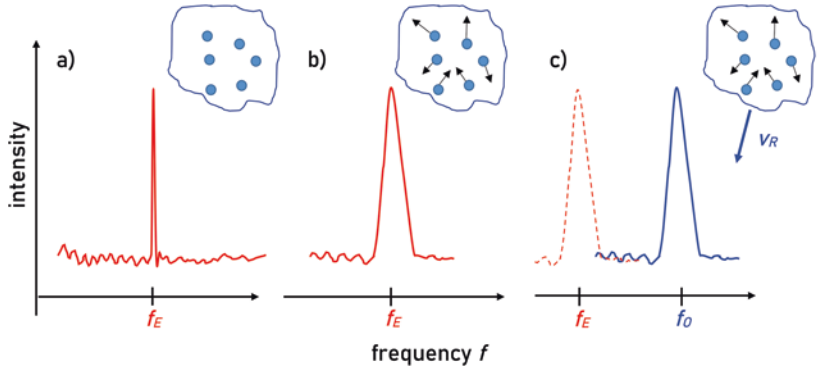

Fig. 2.7 Influence of the Doppler effect on a line spectrum: (**a**) emission of gas atoms at rest (hypothetical), (**b**) Doppler broadened line due to the different motion of the emitting gas atoms relative to the observer, (**c**) Doppler shifted and broadened line due to motion of the emitting gas cloud with radial velocity v_R relative to the observer

addition, e.g. the entire gas cloud and the Earth move towards each other, this broadened line is observed overall at a higher frequency (Doppler shift). For non-relativistic velocities (<10% of the speed of light), only the velocity component in the direction connecting the source and the observer is relevant for the frequency offset, the so-called radial velocity v_R. In astronomy, this is given as a positive value when an object is moving away from the Earth. Since the Doppler effect then leads to a frequency shift towards lower frequencies, the relation between observed frequency f_O, emitted frequency f_E, and radial velocity v_R is given by

$$f_O = f_E\left(1 - \frac{v_R}{c}\right) \tag{2.7}$$

Because of the motion of the Earth around the Sun and that of the Sun around the Milky Way center, the relative velocity of a more distant cosmic source does not remain constant over a year. This must be taken into account when comparing measurements. To do this, the frequency shift is converted to the so-called local standard of rest. This is a coordinate system that moves around the Milky Way

center at the mean velocity of the stars in the vicinity of the solar system. Conversely, the frequency shift makes it easy to demonstrate the proper motion of the Earth through radio astronomical measurements. Examples of measurements of the 21-cm hydrogen radiation are shown in Sect. 4.3.

Summary

Electromagnetic radiation is characterized by frequency, wavelength, polarization and (spectral) intensity.

In addition to thermal radiation, non-thermal processes such as synchrotron radiation also play an important role in cosmic radiation sources. From the dependence of the intensity on the frequency, conclusions can be drawn about the physical cause of the radiation.

In addition, lines appear in the spectrum at certain frequencies which are caused by atomic transitions. The related effects were described based on the 21-cm radiation of hydrogen.

How Does a Radio Telescope Work? 3

3.1 The Components of a Radio Telescope

The components needed by a radio telescope to receive the faint cosmic radio sources and measure their properties are shown in Fig. 3.1.

The receiving antenna of a radio telescope has the purpose, on the one hand, of selecting the area in the sky from which the radiation is to be received and, on the other hand, of concentrating the weak signals from the sources in such a way that they can be further processed by the subsequent electronics. Parabolic reflectors are often used for this purpose, concentrating the incident waves at the focal point. The so-called feed is placed there – the antenna, which converts the waves into an electrical signal. This signal passes through a series of amplifiers and filters. Thus it is limited to the desired frequency range and brought to such a high power level that it can be transferred, to the evaluation electronics, e.g. with a cable or waveguide. There the signals are digitized for further processing. Since they are very weak, they usually have to be averaged or summed up (integrated) over a longer period of time. Depending on the objective of the measurement, a power measurement is then performed or a frequency analysis is carried out to obtain the spectral characteristics of the signal. Based on these data, a representation can then be generated as a curve, map, image, etc. (examples in Chap. 4).

In the simplest case, the feed is placed directly at the focal point of a parabolic antenna (primary focus feed). Depending on the frequency range, typical examples of feeds are dipoles, possibly extended with further elements to form a so-called Yagi antenna, as well as so-called helical and horn antennas.

T. Lauterbach, *Radio Astronomy*, essentials,
https://doi.org/10.1007/978-3-658-36035-1_3

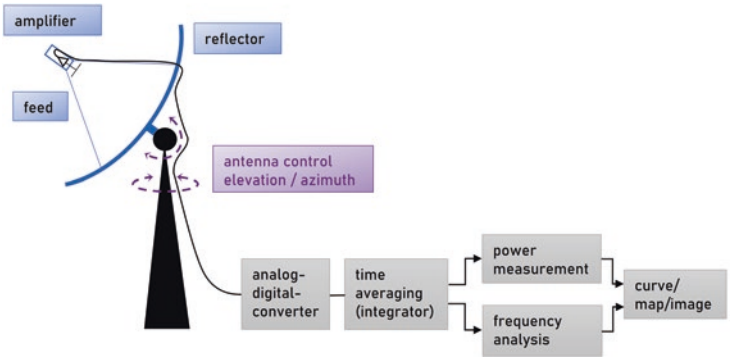

Fig. 3.1 Basic structure of a radio telescope. Blue: receiving antenna with feed and amplifier, grey: signal processing, violet: control system

In a radio telescope, the antenna usually points towards the sky with great elevation. Therefore, thermal radiation from the ground below can hit the feed from the area outside the reflector ("spillover", Fig. 3.5). The feed is therefore constructed in such a way that it receives less well from the edge of the parabolic reflector than from the centre.

Primary Focus Feed of a Radio Telescope

Parabolic mirrors are characterized by the ratio of focal length f to diameter D. A typical value is $f/D \approx 0.4$–0.5 (approximately as in Fig. 3.2). At a larger ratio, the feed attachment would become very long; at a smaller ratio, the required aperture angle of the feed antenna becomes too large. Even at 0.4, the feed antenna must have an aperture angle of about 100°, and the received power in the direction of the edge should be lower by a factor of about 10 than in an area as large as possible in the center. Since such a feed is difficult to manufacture, a secondary reflector is often attached slightly inside the focal point, which reflects the waves into the center of the parabolic reflector, where a feed with a small aperture angle can then be attached (so-called Gregory or Cassegrain beam path, depending on the shape of the secondary reflector).

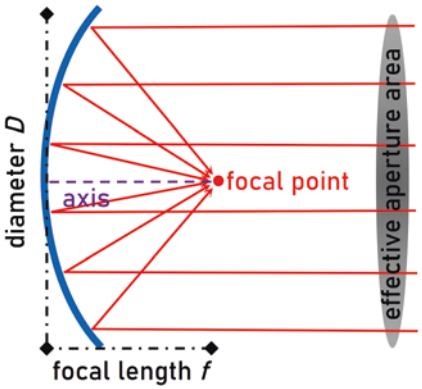

Fig. 3.2 Principle and important quantities of a parabolic reflector (cross-section)

3.2 Properties of a Parabolic Antenna

Receiving antennas are characterized by their effective aperture area A_E. The radiation passing through this hypothetical area is collected by the antenna and is available as electrical power at the antenna terminal if the antenna is optimally aligned and electrically matched. For so-called aperture antennas such as parabolic dishes, the effective area is approximately equal to the geometric area, since all plane waves incident on the aperture are concentrated at the focal point (Fig. 3.2).

Decibel

In radio frequency engineering, power ratios L are expressed in decibels (dB). The conversion formulas are:

$$L = 10\ \text{dB} \cdot \log_{10}\left(\frac{P_1}{P_2}\right) \Leftrightarrow \frac{P_1}{P_2} = 10^{\left(\frac{L}{10\text{dB}}\right)}$$

Due to the uneven use of the parabolic reflector, the effective area is reduced to about 60–80% of the geometric area, depending on the design of the feed. The ratio of effective area to geometric area is called aperture efficiency q. Due to the diffraction at the edge of the reflector, also beams which are not exactly axis-parallel are directed into the focal point. Therefore, if the antenna is moved away from a point source, the received power does not decrease abruptly, but gradually. The angle

between the two directions on either side of the source at which half the power (−3 dB) is still received defines the half-width ϑ of the antenna lobe. The following empirical formula can be found for this (Kark 2010):

$$\vartheta = 62.8^{\circ} \frac{\lambda}{D\sqrt{q}} \tag{3.1}$$

The half-width of the antenna lobe of a 3-m radio telescope is about 5° for the 21-cm radiation of hydrogen, i.e. about 10 full Moon diameters (Fig. 3.3).

Diffraction and other effects cause side lobes of the antenna. From these directions, reception is usually weaker by at least a factor of 100 (20 dB) than from the main direction. When observing weak radio sources, it must be ensured that a strong source, e.g. the sun, is not located in the area of a side lobe.

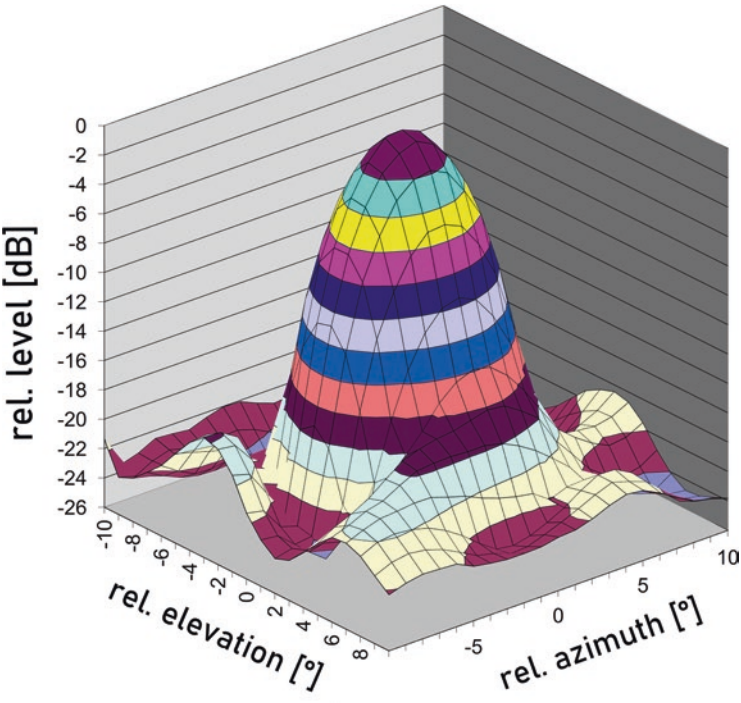

Fig. 3.3 Antenna lobe of the 3 m grating mirror of the Arno-Penzias radio telescope (Fig. 1.6), measured at 1525 MHz. (Image: M. Stöhr, Radio Astronomy Special Interest Group of the Astronomical Society in the European Metropolitan Region Nuremberg)

Questions

What is the half-width of the antenna lobe of a 100 m radio telescope like the one in Effelsberg at a wavelength of 21 cm, if an ideal feed ($q = 1$) were used?

Answer: 8 minutes of arc.

What diameter would the reflector of a radio telescope for 1420 MHz have to have in order to obtain images of radio sources comparable to the optical resolution (at 0.5 µm) of a telescope with 1 m aperture?

Answer: 420 km (same ratio λ/D).

Note: For optical telescopes usually not the half-width is given, but the resolving power, this corresponds to the angular distance from the maximum to the first zero of the antenna lobe. The pre-factor in Eq. 3.1 then increases to 70°.

3.3 Characterisation of the Receiver by the Noise Temperature

In the receiver, as little additional noise as possible should be generated by the electronics so that the weak radio astronomical signals can be detected. Similar to the description of the intensity in Sect. 2.4, the noise can be described by the spectral noise power density $P_{N,f}$ (N for "noise"). This is the noise power related to a frequency interval. For an electrical resistance at temperature T it is ($k_B = 1.38 \cdot 10^{-23}$ J/K is the so-called Boltzmann constant):

$$P_{N,f} = k_B \bullet T \tag{3.2}$$

Example

The noise power spectral density of a resistor at room temperature (290 K) is $4 \cdot 10^{-21}$ W/Hz. ◄

The power at the antenna output can therefore be specified by an equivalent antenna temperature T_A. The noise of the electronic components can also be characterized by a noise temperature. The noise temperature T_V of an amplifier is defined such that the noise power P_V produced by the amplifier without an input signal is

equivalent to that of a (hypothetical) thermal noise source with temperature T_V at the input of the amplifier. The resulting power at the output of the amplifier is then determined by the sum of the temperatures of the antenna and the amplifier: if the amplifier has a power gain G, the output noise power spectral density is given by:

$$P_f = k_B \cdot \left(T_V + T_A\right) \cdot G. \tag{3.3}$$

Background Information

If passive components such as filters, cables or waveguides are used, their attenuation L ("loss") is also related to additional noise. Their noise temperature T_L is given by:

$$T_L = T_0 \left(\frac{1}{L} - 1 \right). \tag{3.4}$$

T_0 is the (absolute) temperature of the passive component, usually 290 K. A (long) antenna cable with $L = 0.25$ (6 dB attenuation), for example, has a noise temperature of 870 K.

If several components, which are characterized by their amplifications G_i or attenuations and their noise temperatures $T_{V,i,}$ are connected in series, their total noise temperature $T_{V,\mathrm{tot}}$ is calculated by the so-called Friis' formula:

$$T_{V,\mathrm{tot}} = T_{V,1} + \frac{T_{V,2}}{G_1} + \frac{T_{V,3}}{G_1 G_2} + \ldots + \frac{T_{V,n}}{G_1 G_2 \ldots G_{n-1}} \tag{3.5}$$

where L replaces G for passive components. The noise temperature $T_{V,1}$ of the first component after the feed is therefore decisive for the total noise temperature. In addition, it should have a high amplification $G_{1,}$ so that the noise temperatures of subsequent components, especially passive components, do not have a strong effect.

Manufacturer's Specifications of Radio Frequency Components

In order to be able to calculate the noise temperature of a receiver, the specifications found in data sheets of electronic components must be converted accordingly. For amplifiers, this is usually the gain G and the noise figure F, each given in decibels. The conversion to G and T_V is done with:

$$G = 10^{\left(\frac{G}{10\,\mathrm{dB}}\right)} \text{ and } T_V = T_0 \left[10^{\left(\frac{F}{10\,\mathrm{dB}}\right)} - 1 \right]. \tag{3.6}$$

The attenuation of passive components is usually specified as an attenuation value L in decibels. Although attenuations lead to a weakening of the signal, the decibel value usually does not include the correct negative sign, but e.g. "cable attenuation 6 dB". The attenuation L then results from:

$$L = 10^{\left(\frac{-L}{10\,\mathrm{dB}}\right)} . \tag{3.7}$$

Calculation Example for Noise Temperature

At the focal point of the Arno Penzias Radio Telescope (Fig. 1.6), there is a short coaxial cable with 0.2 dB attenuation between the feed antenna and the first amplifier, corresponding to (Eq. 3.7) $L = 0.955$ and (Eq. 3.4) $T_1 = 13.7$ K. The amplifier has G =14.2 dB and $F = 0.47$ dB, corresponding to (Eq. 3.6) $G_2 = 26.3$ and $T_{V,2} = 33.2$ K. A filter with 2 dB passband attenuation follows, so $L_3 = 0.63$ and $T_3 = 170$ K. After another amplifier there is a 10 m long antenna cable with 3.7 dB attenuation, corresponding to $L_4 = 0.42$ and therefore $T_4 = 405$ K. This results according to Eq. 3.5:

$$T_{V,\mathrm{tot}} = 13.7\,\mathrm{K} + \frac{33.2\,\mathrm{K}}{0.955} + \frac{170\,\mathrm{K}}{25.1} + \frac{33.2\,\mathrm{K}}{15.8} + \frac{405\,\mathrm{K}}{416} = .$$

$$= 13.7\,\mathrm{K} + 34.8\,\mathrm{K} + 6.8\,\mathrm{K} + 2.1\,\mathrm{K} + 0.97\,\mathrm{K} = 58.4\,\mathrm{K}$$

Interpretation

As can be clearly seen, the short cable between feed and amplifier (13.7 K) and the first amplifier (34.8 K) contribute significantly to the total noise temperature, the subsequent components do not play a major role because of the high gain. However, the second amplifier is absolutely necessary to keep the influence of the cable attenuation of the long antenna cable low, otherwise this would provide a contribution of 25.6 K.

3.4 Signal Processing and Display

After passing through the amplifier and filter chain, the received signal is digitized by a "Software Defined Radio" (SDR) with fast and high-resolution analog-to-digital converters. The digitized signal is further processed on a computer. For example, the total received power in a given bandwidth or a frequency spectrum can be calculated. To reduce the fluctuation of the weak signals, they usually have to be averaged over a longer period of time (e.g. a few seconds).

Example of Digital Signal Processing

Digital signal processing is explained by means of the reception of the 21-cm radiation from the constellation Cassiopeia with the 1.5 m radio telescope (Fig. 1.6). The signal from the antenna is amplified and filtered. This analog signal *x(t)* is applied to the SDR for digitization.

The sampling rate of the SDR must be set to at least twice the desired bandwidth according to the so-called Nyquist theorem. The gain of the SDR must be selected in such a way that the A/D converters are well controlled.

The sampled values (Fig. 3.4, left picture) from the SDR are further processed in a PC. For this purpose, they are divided into blocks (of e.g. 1024 values each) and converted block by block into the frequency domain using a so-called Fast Fourier Transform (FFT) (Fig. 3.4, middle image). The block length corresponds to the number of values in the spectrum. Therefore, the longer the blocks of samples, the better the frequency resolution. The strong line in the middle of the spectrum is an interference line caused by the receiver concept of the SDR used. The frequency range of the spectrum to be displayed is "cut out". The values of temporally successive cutouts are averaged over the desired measurement time using a suitable algorithm, e.g. Welch's algorithm (Welch 1967). This greatly reduces the fluctuations of the values, as can be seen from the comparison of the spectra when averaged over 20 ms and 3 s (Fig. 3.4, right figure). The spectral distribution of the hydrogen radiation becomes recognizable and can be evaluated, for example, with regard to the Doppler shift.

For details on digital signal processing, please refer to the literature (e.g., Heuberger and Gamm 2017).

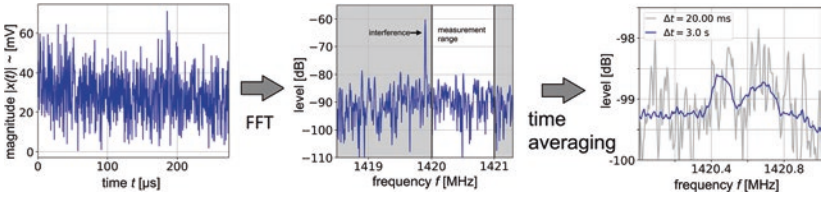

Fig. 3.4 Digital signal processing for displaying the frequency spectrum in the range of the 21-cm radiation, see text. (Image: H. Lieske, Radio Astronomy Special Interest Group of the Astronomical Society in the European Metropolitan Region Nuremberg)

3.5 Determination of the Radiation Temperature and Intensity of a Cosmic Source

The issue of determining the intensity of a cosmic source is shown in Fig. 3.5. In addition to the signal from the source with equivalent radiation temperature T_S, which leads to an antenna temperature $T_{A,S}$, a radiation background with T_B also impinges on the receiving antenna. Under this term, the galactic radiation, the 3 K background radiation, the thermal radiation from the Earth's atmosphere and, if applicable, the "spillover" of the feed are summarized here for simplification. In total, this results in the antenna temperature $T_{A,\mathrm{tot}}$. During the measurement, the noise of the receiver, characterized by T_R, is added to this.

The temperatures T_B and T_R as well as the bandwidth gain product $B \cdot G$ of the receiver must be known in order to calculate the cosmic source contribution from the total measured power. For this purpose, one can proceed as follows:

- T_B can be determined from a measurement "past the source" (spatially or in terms of frequency).
- T_R can be calculated or measured from amplifier data, etc., see the calculation example in Sect. 3.3.

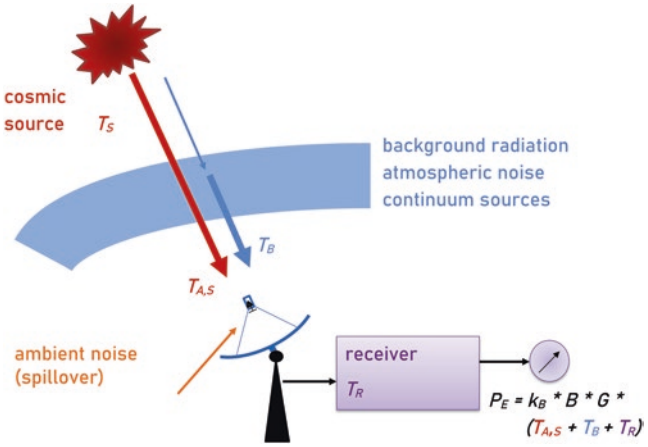

Fig. 3.5 Situation when receiving the signal from a cosmic source

- $B \cdot G$ can be determined from a calibration measurement, e.g. by directing the antenna to an area whose temperature and emissivity are known (cosmic reference source, absorber of known temperature). Alternatively, an electronic noise source of known power can be connected to the amplifier input instead of the feed. In order to take into account a change in the gain, e.g. due to a temperature drift, the antenna and the noise source are continuously switched over during the measurement (so-called Dicke radiometer).

Once these quantities have been determined, the antenna temperature $T_{A,S,}$ which is caused by the source alone, can be calculated:

$$T_{A,S} = T_{A,tot} - T_B = \frac{P_E}{k_B \cdot G \cdot B} - T_R - T_B \tag{3.8}$$

The spectral intensity related to the antenna temperature $T_{A,S}$ then can be calculated from

$$S_f = \frac{2k_B T_{A,S}}{A_E}$$

The so-called brightness temperature of the source T_s depends on how the areal extent (described by the so-called solid angle Ω_s) of the source compares to the the solid angle covered by the antenna lobe (Ω_A). The following relationships apply (Burke et al. 2019, p.76 ff):

- compact source (extent smaller than the area covered by the antenna lobe, e.g. the Sun in a 3 m radio telescope):

$$T_S = \frac{\Omega_A}{\Omega_S} T_{A,S}$$

- large-area source (extension larger than the area covered by the antenna lobe, e.g. cosmic background radiation):

$$T_S = T_{A,S}$$

Example: Determination of the Equivalent Radiation Temperature of the 21-cm Radiation from the Constellation Cassiopeia

Using the 1.5 m parabolic dish (Fig. 1.6), two measurements were made with otherwise identical settings in the direction of the observatory wall and in the direction of the constellation Cassiopeia. Even though a building wall cannot be

considered an absorber at 1.4 GHz because it has a significant reflectance, it can be assumed that in this direction thermal radiation at ambient temperature is measured. From two measured values, once at the frequency of 21 cm radiation and once at a higher frequency (Fig. 3.6), the different quantities were determined.

For the evaluation we consider the measurement results of both measurements at 1420.9 MHz for the background and at 1420.35 MHz for the hydrogen spectrum. The background value under the hydrogen spectrum is extrapolated from the value at 1420.9 MHz analogous to the measurement of the thermal radiation of the observatory wall, since the same frequency response is to be expected due to the digital filtering in the SDR receiver.

When measuring in the direction of the observatory it was assumed that:

- Ambient temperature: 273 K,
- Receiver noise temperature (calculated as in Sect. 3.3): $T_R = 67$ K.

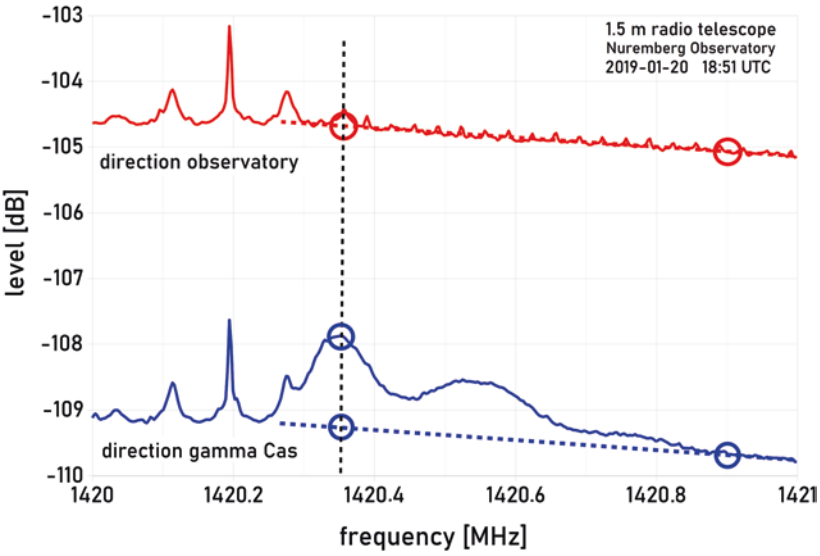

Fig. 3.6 Measurement to determine the radiation temperature of the 21 cm hydrogen radiation, measurement duration 40 s. Upper curve: radio telescope directed to the wall of the observatory, lower curve: radio telescope directed to γ Cas. The signals below 1420.3 MHz are interference lines

Then the antenna temperature at the measurement towards the observatory is $T_{A,\mathrm{ref}} = 340$ K and from the measured power $P_{A,\mathrm{ref}}$ (1420.35 MHz) = −104.75 dB we can calculate analogously to Eq. 3.8:

$$k_B \cdot G \cdot B = \frac{P_{A,\mathrm{ref}}}{T_{A,\mathrm{ref}}} = 1.0 \cdot 10^{-13}\,\mathrm{W/K}.$$

In the γ Cas direction, the received background power (extrapolated from 1420.9 MHz) is P_B (1420.35 MHz) = −109.3 dB and from this we calculate analogously to Eq. 3.8:

$$T_B = \frac{P_B}{k_B \bullet G \bullet B} - T_R = 118\,\mathrm{K} - 67\,\mathrm{K} = 51\,\mathrm{K}$$

The total power with the source is $P_{A,\mathrm{tot}}$ (1420.35 MHz) = −107.9 dB. Now Eq. 3.8 can be fully applied and gives

$$T_{A,S} = \frac{P_{A,\mathrm{tot}}}{k_B \bullet G \bullet B} - T_R - T_B = 163\,\mathrm{K} - 67\,\mathrm{K} - 51\,\mathrm{K} = 45\,\mathrm{K}$$

Since the source is large-area, this is also the radiation temperature of the source. The result is in good agreement with the published value of 47 K (Kalberla et al. 2005). This corresponds to a spectral intensity of $2.8 \bullet 10^6$ Jy.

3.6 Antenna Control

The antenna must be pointed in the direction of the source to be observed. Usually the antennas of radio telescopes are rotated around a vertical axis to adjust the direction (azimuth) and around a horizontal axis for the altitude adjustment (elevation). This corresponds to the azimuthal mount of an optical telescope. The position of a source is, for example, known in the moving equatorial system (right ascension α, declination δ) or in galactic coordinates (galactic longitude and latitude ℓ, b) and must be converted to the instantaneous direction and altitude. Formulas for this can be found in textbooks of astronomy (e.g. Hanslmeier 2014, Chapter 1).

If measurements are to be made over a longer period of time, the direction of the antenna must follow the movement of the sources in the sky. With very simple facilities, but also with the largest radio telescopes (Arecibo, FAST) one does without the movement of the antenna. One uses then the earth rotation and if necessary a shift of the feed, in order to seize the different ranges of the sky in the course of a day.

How Does a Radio Telescope Work?

Radio telescopes focus the radiation incident on a large area. A parabolic reflector is often used for this purpose. A feed antenna converts the focused radiation into an electrical signal. Its noise power spectral density is described by the antenna temperature. Simultaneously with the source, a noise background and the receiver noise are measured. Through various measurements and calculations, the contribution of the source to the noise power can be isolated and from this its spectral intensity can be calculated.

What Can You Observe with a Radio Telescope?

4

4.1 Radio Radiation from the Sun

As explained in Chap. 2, the Sun is the strongest cosmic radio source. Its radiation is therefore comparatively easy to receive. It can be used to check the function of the antenna control and the receiver sensitivity. For this purpose, the antenna is aligned exactly to the south (azimuth 180°) and the expected altitude of the sun at noon is set as elevation. If one records the received radiation in a suitable period around true noon, the received power increases when the sun is detected by the antenna lobe, reaches the maximum exactly at the time of true noon at the receiving location and decreases again afterwards (Fig. 4.1). A similar result is obtained when the antenna is slewed over the position of the sun.

The intensity of solar radiation can be used to draw conclusions about solar activity. For this purpose, the spectral intensity of the solar radiation (the so-called solar flux) is measured at 2.8 GHz (10.7 cm wavelength). The value is given in so-called solar flux units (sfu), 1 sfu corresponds to 10^4 Jansky. Typical values are between 70 sfu at sunspot minimum and over 200 sfu during phases of greatest solar activity. Several stations worldwide carry out daily measurements of solar flux and publish the data on the Internet, e.g. Natural Resources Canada.

T. Lauterbach, *Radio Astronomy*, essentials,
https://doi.org/10.1007/978-3-658-36035-1_4

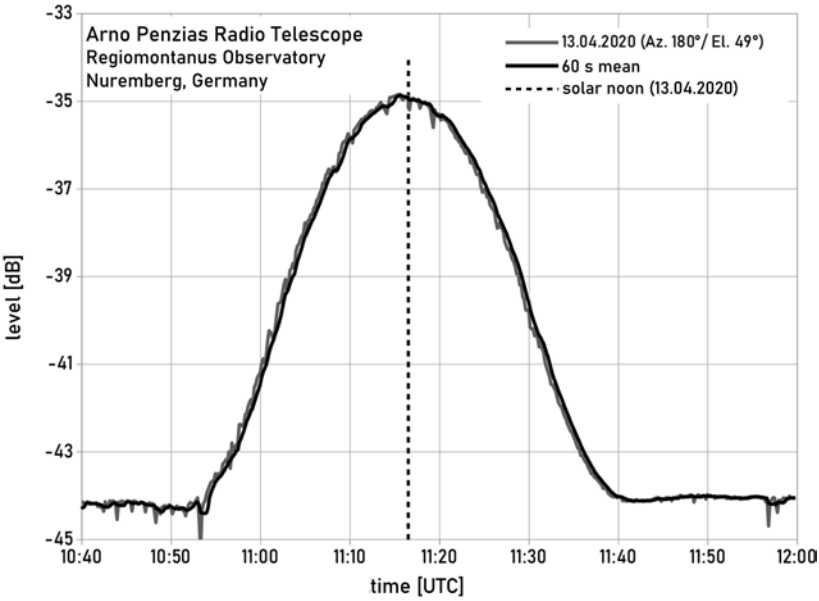

Fig. 4.1 Measurement of the intensity of solar radiation at 1400 MHz with the 3-m radio telescope of the Nuremberg Observatory, see text. With correctly adjusted antenna the signal level reaches the maximum at the time of solar noon

4.2 The Cassiopeia A Radio Source

This radio source is one of the strongest after the sun, but at 1.4 GHz it is weaker by a factor of about 1000 (Fig. 2.5). Therefore, the question arises whether the resulting significantly smaller difference in antenna temperature compared to the radiation background can be detected, since the signals are indeed subject to noise. It is necessary to increase both the averaging time and the bandwidth of the power measurement. Then, even with a small radio telescope, the radiation can be well distinguished from the background, as Fig. 4.2 shows.

The radiometer equation (Kraus 1966, p. 102) links the minimum measurable temperature difference ΔT to the bandwidth B, the averaging time Δt and the number of measurements N. T_{sys} is the system temperature (antenna temperature + noise temperature of the receiver).

$$\Delta T \approx \frac{T_{sys}}{\sqrt{B \cdot \Delta t \cdot N}}$$

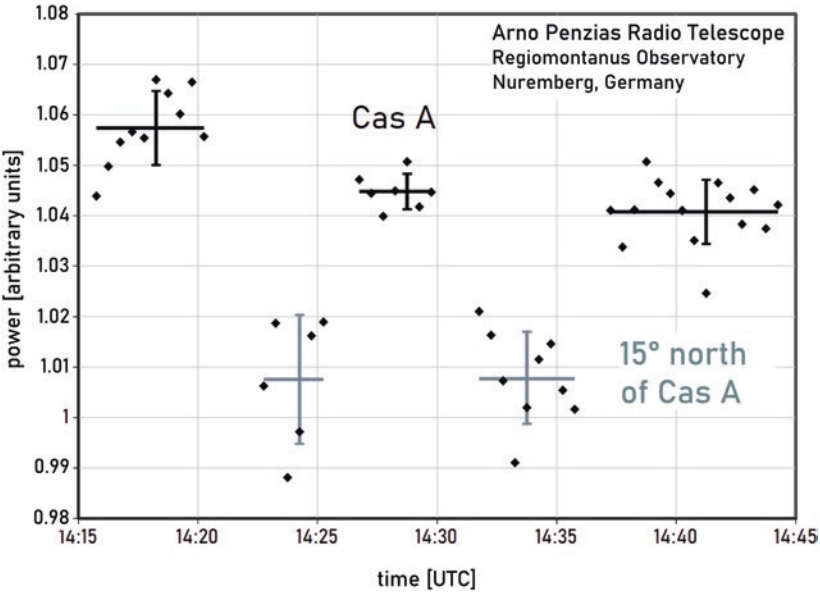

Fig. 4.2 Measurement of the continuum radio emission from Cassiopeia A at 1417 MHz. The antenna was slewed approximately every 5 min between the position of the source and a celestial region with the same elevation but 15° larger azimuth (i.e. 15°further north, since the source was located in the northwest). Several of the 30 s single measurements (diamonds) with bandwidth 135 kHz were averaged again (lines) to show the difference in received power of only about 3%. The vertical bars indicate the range of ± one standard deviation

Questions

For a single measurement with 2 kHz bandwidth, what integration time is required to measure the (approximately point-like) source Cas A at 1420 MHz with a 3-m radio telescope (with $q = 0.7$)? The spectral intensity is $5 \bullet 10^3$ Jy. For the receiver noise temperature and the sky temperature, use the data from the example in Sect. 3.4.

Answer: From the formula for the relationship between spectral intensity and antenna temperature for point sources given in Sect. 3.5, $\Delta T = T_{A,Q} = 9$ K. From the radiometer equation, $\Delta t = 0.1$ s.

4.3 The 21-cm Radio Radiation from the Milky Way

The formation of the 21-cm radio radiation by the hyperfine structure transition of the neutral hydrogen atoms was described in Sect. 2.5.3. In the Milky Way, atomic hydrogen exists mainly in the regions between the stars. Therefore, by observing this radiation and its Doppler shift, one can make statements about the motion of the different regions of the Milky Way relative to each other. For the interpretation of the measurements it is helpful to have the structure of the Milky Way in mind (Fig. 4.3).

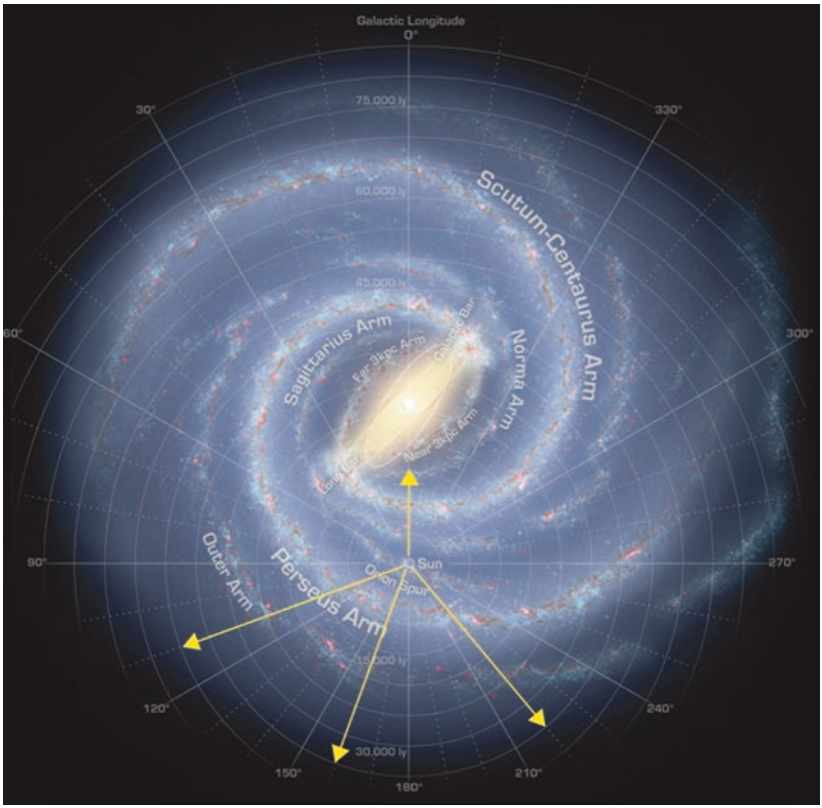

Fig. 4.3 Artist's impression of the Milky Way from a direction perpendicular to the galactic plane from the outside. The bar-shaped centre and the spiral arms can be seen. The Sun is located at a distance of about 25,000 light-years from the galactic center ("Sun"). The arrows refer to the directions of the measurements shown in Fig. 4.5. (Credit: NASA/JPL-Caltech/R. Hurt (SSC/Caltech))

The different directions with respect to the Milky Way are given in galactic coordinates. The galactic longitude ℓ indicates the angle to the galactic center in the galactic plane ("Galactic Longitude" in Fig. 4.3). The galactic latitude b is the angle to the galactic plane.

Depending on the direction from which the radiation comes, it is subject to different Doppler shifts, since most objects (stars, gas clouds) move approximately on circular paths around the center. Surprisingly, the rotational velocity in the Milky Way at some distance from the center hardly depends on the distance anymore (Burke et al. 2019, p. 344) and is about 225 km/s. This cannot be explained by *Newton's* law of gravity and is attributed to the effect of so-called dark matter, which is currently being searched for intensively.

Using the example of Fig. 4.4, it can be seen that this rotational behaviour of the Milky Way results in a radial velocity of the radiation sources S relative to an observer O, e.g. at the location of the Sun. The velocity vectors of the sources and the observer (gray) can each be decomposed into a radial component in the direction of the line connecting them (colored) and one perpendicular to it (not shown in the figure). In this example, for source S_1 in the direction of the Milky Way's rotational motion this results in a negative relative radial velocity (v_{R1}, toward the receiver)

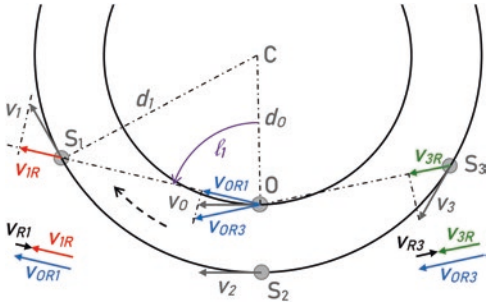

Fig. 4.4 Geometry of a simple model to explain the Doppler shift in the observation of 21-cm radiation from the Milky Way arms. The different direction of motion results in a radial velocity between different sources and a receiver, which move on circular paths around the common center C, see text

and thus a Doppler shift to higher frequencies. In contrast, for source S_3 from the opposite direction, there is a positive radial relative velocity (v_{R3}) and thus a Doppler shift to lower frequencies. For source S_2 in the direction opposite to the center, no velocity component occurs in the direction of the connecting line and thus no Doppler shift.

Background Information

In general, the radial velocity between the observer O and, for example, the source S_1 with galactic length ℓ_1 and distance d_1 from the center C can be calculated from the geometry of Fig. 4.4 by (Voigt 2012, p. 728):

$$v_{R1} = d_O \left(\frac{v_1}{d_1} - \frac{v_O}{d_O} \right) \sin l_1 \tag{4.1}$$

From this it follows that the radial relative velocity is zero for all sources which have the same distance from the galactic center as the observer (under the condition $v_1 = v_O$) because of the term in parenthesis being zero independently of the galactic longitude, likewise for sources at $\ell_1 = 0°$ and 180° because of the sine function being zero independently of the distances. For all other sources the sign changes at these galactic longitudes.

For sources with $d_1 > d_O$, the term in parenthesis is always negative, resulting in the following situation: sources in the direction of the rotation of the Milky Way ($\ell_1 < 180°$) have negative, sources with $\ell_1 > 180°$ have positive radial relative velocities. For sources in the range $\ell_1 = 90°$ ... 270° this is always true, since in this range one is looking outward in the Milky Way as seen from the Sun or Earth (Fig. 4.3); in the remaining range it is true for sources farther from the center than the observer, as in the example of Fig. 4.4.

For sources with $d_1 < d_O$, the term in parenthesis is positive and therefore the situation is exactly reversed.

In addition, there is a seasonal Doppler shift due to the motion of the Earth around the Sun, which is not in the galactic plane.

The observations of the 21-cm line confirm these considerations (Fig. 4.5). All examples are measured in the galactic plane, i.e. at latitude 0°.

The frequency was converted into the radial velocity by Eq. 2.7, the correction to the local standard of rest was omitted. One observes practically no radial velocity in the direction of the galactic center, negative radial velocities in directions 100° and 140°, and positive radial velocities in direction 220°. In most directions several lines appear, which show different radial velocities, this indicates the origin of the radiation from differently distant areas of the Milky Way, e.g. different Milky Way arms, since then according to Eq. 4.1 the radial velocities and thus the Doppler shifts are

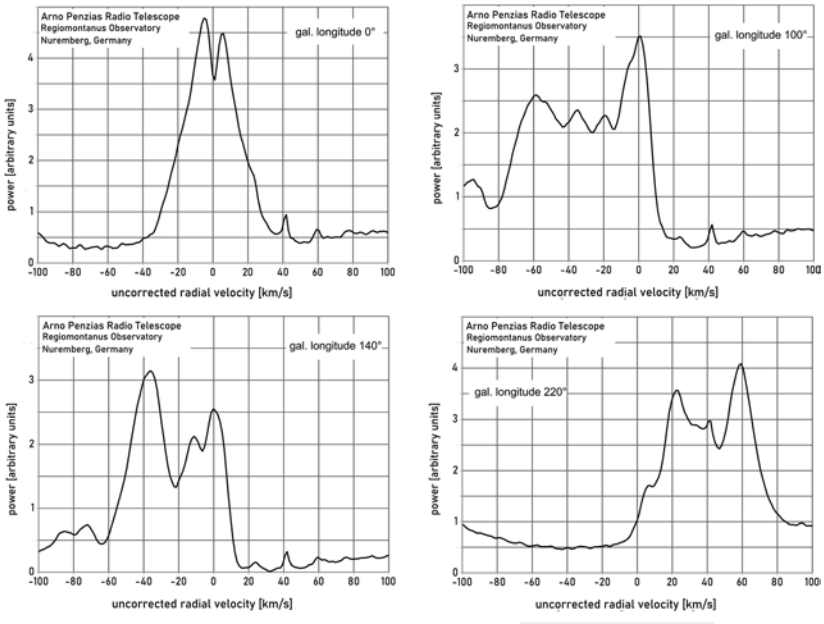

Fig. 4.5 Measurements of 21-cm radiation from different regions of the Milky Way with the 3-m radio telescope (Fig. 1.6)

different. This can also be seen in Fig. 4.3. With such measurements, the spiral arm structure of the Milky Way was already recognized in the 1950s (Oort 1959).

The measurement in direction 0° shows a special feature. The hydrogen line there is not only to be seen as an emission line, as in the other measurements, but also as an absorption line. The strong radiation from the galactic center is partly absorbed again by the gas in the arms in front of it. This leads to the "notch" at radial velocity 0.

4.4 Creation of Radio Maps

In order to get a visual impression of the distribution of the 21-cm radiation, the data of many individual measurements can be combined to form an image and the various properties such as strength and frequency can be coded by color and brightness. By means of digital image processing like mean value corrections etc. the

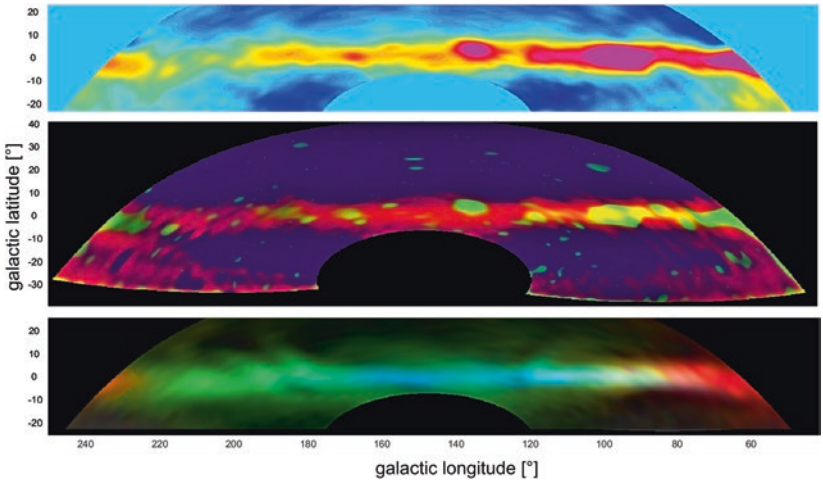

Fig. 4.6 Color-coded radio maps in the 21-cm radiation range, made with measurements from a 2.65-m radio telescope. Top: total intensity over the full bandwidth (8 MHz), middle: Intensity of continuum (green) and hydrogen (red) radiation shown separately, bottom: Intensity of hydrogen radiation only, color coding: Doppler shift. Filter: unsharp mask. (Images: Johannes Ebersberger, Radio Astronomy Special Interest Group of the Astronomical Society in the European Metropolitan Region Nuremberg)

influences of e.g. the temperature drift of the receiving system and the different contributions of atmospheric radiation e.g. by clouds (Sect. 3.5) can be taken into account and corrected. Examples of maps produced with an amateur radio telescope are shown in Fig. 4.6, where it becomes clear that radiation from the Milky Way dominates by far. Spectral filtering can be used to separate the radiation from atomic hydrogen from the continuum of, for example, Cas A and Cyg A. In addition, color coding of the Doppler shift of the hydrogen line can be used to visualize the regions that have a positive or negative radial velocity (Ebersberger 2020).

Summary

Even with small radio telescopes, the radiation from the Sun, the brightest radio sources and the 21-cm radiation from the Milky Way can be observed. From this, conclusions can be drawn about the rotation of the spiral arms of the Milky Way.

Outlook

5

5.1 Interferometry

The large radio telescopes of the scientific institutions do not function in themselves in a different way than described in Chap. 3. Due to the much larger antenna effective area, which increases with the square of the diameter, a 100 m radio telescope could detect signals which are weaker by a factor of 1100 compared to a 3 m dish. Amplifiers with lower noise temperatures, achieved e.g. by cooling, can further increase the sensitivity. With appropriately long integration time and bandwidth, observations of sources with intensities of milli-Jansky and below become possible. However, according to Eq. 3.1, the angular resolution remains limited to several arc minutes. Since the diameter of a radio telescope cannot be increased arbitrarily, another technique must be used to improve the resolving power: interferometry.

The principle is shown schematically in Fig. 5.1. The simultaneously received signals from two (or more) radio telescopes at the distance of the baseline B are combined, e.g. added or multiplied. This results in a diagram with many individual narrow lobes instead of the broad antenna diagram of a single antenna (Fig. 5.2). The angular spacing of the maxima of this interference pattern is determined by the ratio of the length of the baseline B to the wavelength λ. The larger the ratio B/λ, the narrower are and the closer are the lobes of the common pattern. Since with antennas at an angle, as in Fig. 5.1, the waves strike the antenna that is in front in the direction of reception earlier, the signal from this antenna must be delayed so that the same interference pattern as in Fig. 5.2 occurs in each case.

T. Lauterbach, *Radio Astronomy*, essentials,
https://doi.org/10.1007/978-3-658-36035-1_5

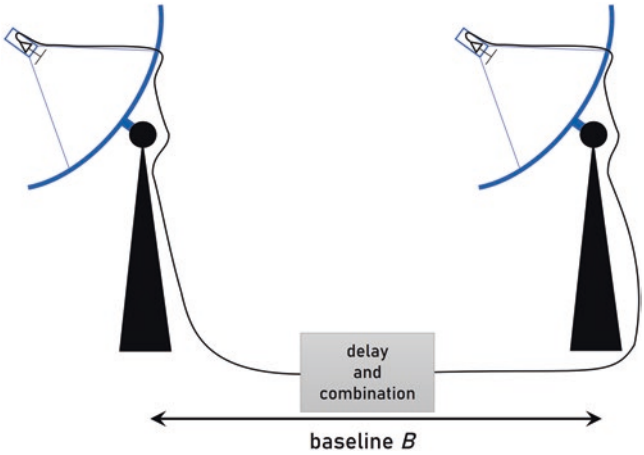

Fig. 5.1 Principle of a radio interferometer with two identical antennas at a distance B

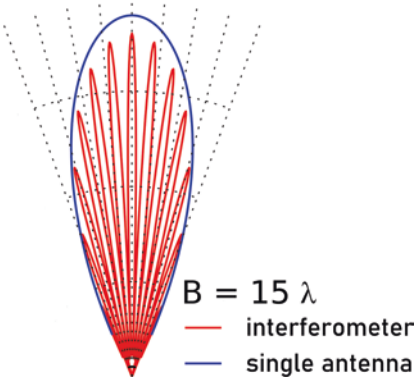

Fig. 5.2 Schematic antenna diagram of a single antenna and an interferometer consisting of two identical antennas with a baseline of 15 wavelengths in the direction perpendicular to the baseline

Since the splitting of the diagram only occurs in the direction of the baseline, a two-dimensional image of a radio source requires two interferometers with baselines arranged perpendicular to each other, i.e. at least 3 radio telescopes. In order to completely capture the structure of a source, baselines of different lengths are also required. Therefore, either many antennas are placed along different directions or are movable on rails, for example. A typical example of a radio interferometer is the Very Large Array (VLA), Fig. 5.3, in New Mexico, USA, which consists of 27 active antennas, each 25 m in diameter, arranged along three lines in a Y-shape. The spacing of the antennas can be varied between 1 and 37 km. In the frequency range around 50 GHz, this results in an angular resolution of 0.04 arc seconds. Compared to the approximately 0.9 arc minutes of a single antenna according to Eq. 3.1, this means an improvement in resolution by a factor of 1350.

Fig. 5.3 The Very Large Array radio interferometer with a total of 27 active antennas. (Credit: NRAO/AUI/NSF)

For interferometry it is not necessary to combine the signals of the different antennas directly at reception. They can also be recorded individually and combined later. For this, however, it is necessary that time signals with correspondingly high accuracy, e.g. from atomic clocks, are also recorded. In this case, the radio telescopes involved can even be located on different continents. This is known as "Very Long Baseline Interferometry" (VLBI). The angular distance that can be resolved with two radio telescopes at a distance of 7500 km is again about a factor of 200 smaller than with the VLA. This allows the structures of cosmic sources to be studied with a high level of detail. An even greater resolution could be achieved if radio telescopes were brought into space, where even longer baselines could be realized and even shorter wavelengths used.

Since the superimposed signal in interferometers depends sensitively on the exact distance between the antennas, VLBI can be used to accurately measure baselines several thousand kilometres long with radio sources such as quasars. This can even be used to observe continental drift, e.g. the annual divergence of Europe and North America by about 17 mm (Burke et al. 2019, p. 287). Radio telescopes are therefore also used for precision geodetic measurements, e.g. that of the Geodetic Observatory at Wettzell, Germany. There, VLBI is used to determine the orientation of the Earth in space and its rotational speed on a weekly basis to ensure the accuracy of satellite navigation systems.

5.2 Radio Astronomical Research

With the method of interferometry it is possible to resolve and display the structures of astronomical radiation sources. This leads to a number of discoveries which are not possible with optical observations alone or which complement them. Some of these have already been mentioned in the introduction (Sect. 1.4) and as examples of cosmic sources (Sect. 2.5). Many other findings from the history of radio astronomy and from current research can be found on the websites of the radio astronomical institutes and the major radio telescopes, e.g. the Max Planck Institute for Radio Astronomy in Bonn, Germany, the Jodrell Bank Centre for Astrophysics at the University of Manchester, U.K. and the US National Radio Astronomy Observatory. A list of radio telescopes can be found in Wikipedia. Recent (2019–2020) publications and press releases from the above

institutions deal with, for example, the measurement of the wind speed on a brown dwarf star, with details of the quasar 3C 279, with accretion disks around stars in which planets are formed, with massive neutron stars, radio bursts, pulsars, the destruction of a star in the gravitational field of a supermassive black hole, with detailed studies on the black hole in the center of our Milky Way, and with the verification of predictions of general relativity and cosmological models. This exemplifies the wide field of radio astronomical research, which contributes to practically all questions of modern astronomy, cosmology and physics. In particular, the research topics of modern radio astronomy lie in the following areas (Burke et al. 2019, Part III):

- Properties of the sun and its dynamics, e.g. radiation bursts,
- Properties of the solar corona,
- Exploration of the planets by radar measurements, determination of surface temperatures of the planets, measurement of radiation from their magnetic fields (especially for Jupiter),
- Investigation of the thermal and non-thermal radiation of stars, of dust clouds and accretion disks,
- Molecular clouds around stars, in particular "red giants", in which radiation is produced by stimulated transitions in OH, H_2O, CH_3OH and SiO (MASER),
- Stellar explosions (novae, supernova remnants),
- X-ray binaries,
- Spiral structures of the Milky Way and other galaxies, rotation curves,
- Investigation of the center of the Milky Way (black hole, central molecular zone),
- Magnetic fields in the Milky Way and other galaxies,
- Structure, magnetic fields, rotation of neutron stars (pulsars),
- Radiation of gravitational waves by double neutron stars,
- Active galactic nuclei with supermassive black holes (quasars, radio galaxies, blazars),
- Properties of the cosmic background radiation, temperature anisotropy, angular distribution, polarization, and from these the derivation of cosmological quantities,
- Observation of gravitational lensing.

5.3 Own Entry into Radio Astronomy

Besides research at universities and large-scale research institutions, basic radio astronomical observations are also possible for interested laymen. There are a number of suggestions on the Internet on how to set up simple radio telescopes and use them to observe, for example, the radiation of the Sun and the 21-cm radiation of hydrogen (Fritzsche et al. 2006; Leech 2013; Ebersberger 2017). Some radio telescopes decommissioned as research facilities continue to be operated by associations and can be visited (Astropeiler Stockert, Germany, Dwingeloo Radio Telescope, The Netherlands). Some public observatories also operate radio telescopes and introduce visitors to radio astronomy (Fig. 1.6, Chap. 4). Valuable information may be obtained e.g. from the Website of the Society of Amateur Radio Astronomers (SARA). There you will also find links to radio astronomy experiments that can be performed with amateur means. Another easy way to get started in radio astronomy is to use web receivers for radio astronomical signals. A 2.3-m radio telescope for 21-cm radiation ("SALSA"), which is accessible via the Internet and with which one can carry out one's own measurements free of charge after prior registration, is located at the Swedish Space Observatory in Onsala.

Summary

Through interferometry, a much higher resolution can be achieved than with individual radio telescopes. This allows radio astronomical research to contribute to many current questions in astronomy, cosmology and physics.

But even beyond research, there are many opportunities to get involved with radio astronomy.

Sources and Literature

General Introductions to Astronomy (Selection)

Hanslmeier, Arnold 2016. Faszination Astronomie, Berlin, Heidelberg: Springer, 2. Aufl.

Hanslmeier, Arnold 2014. Einführung in Astronomie und Astrophysik, Berlin, Heidelberg: Springer, 3. Aufl.

Voigt, Hans-Heinrich 2012. Abriss der Astronomie, Herausgeg. von H.-J. Röser und W. Tscharnuter, Weinheim: Wiley-VCH, 6. Aufl.

Barbieri, Cesare, Ivano Bertini, 2021. Fundamentals of Astronomy, Boca Raton, Fl: CRC Press

Kartunen, Hanno, Pekka Kröger, Heikki Oja, Markku Poutanen, Karl Johan Donner (Eds.) 2017. Fundamental Astronomy. Berlin, Heidelberg: Springer, 6th Ed.

Inglis, Michael, 2015. Astrophysics Is Easy. Cham, Heidelberg, New York, Dortrecht, London: Springer 2nd. Ed.

Marov, Mikhail Ya. 2015. The Fundamentals of Modern Astrophysics, New York, Heidelberg, Dortrecht, London: Springer

Books on Radio Astronomy (Selection)

Kraus, J.D. 1966. Radio Astronomy, New York: McGraw-Hill

Burke, Bernard F., Francis Graham-Smith, Peter N. Wilkinson 2019. An Introduction to Radio Astronomy, Cambridge: Cambridge University Press, 4. Aufl.

Wilson, Thomas, Susanne Hüttemeister 2013. Tools of Radio Astronomy: Problems and Solutions, Berlin, Heidelberg: Springer.

Marr, Jonathan M., Ronald L. Snell, Stanley E. Kurtz 2015. Fundamentals of Radio Astronomy: Observational Methods, Boca Raton: CRC Press.

T. Lauterbach, *Radio Astronomy*, essentials,
https://doi.org/10.1007/978-3-658-36035-1

Snell, Ronald L., Stanley Kurtz, Jonathan Marr 2019. Fundamentals of Radio Astronomy: Astrophysics, Boca Raton: CRC Press.
Condon, James J., Scott M. Ransom 2016. Essential Radio Astronomy, Princeton: Princeton University Press, (also available online: https://science.nrao.edu/opportunities/courses/era).
Baars, Jacob W.M., Hans J. Kärcher 2018. Radio Telescope Reflectors, Historical Development of Design and Construction, Berlin, Heidelberg: Springer.

Chapter 1

Algeo, John, Adele S. Algeo (Hrsg.) 1993. Fifty Years Among the New Words: A Dictionary of Neologisms 1941–1991, Cambridge: Cambridge University Press.
Bahr, Charles, Marcus Weldon, Robert W. Wilson 2014, The Discovery of Cosmic Microwave Background, Bell Labs Technical Journal, Vol. 19, p. 1.
Bouman, Katherine L. 2020. Portrait of a Black Hole, IEEE Spectrum, February 2020, p. 22.
Haystack Small Radio Telescope, https://www.haystack.mit.edu/edu/undergrad/srt/index.html, accessed 23.03.2020.
https://www.mpifr-bonn.mpg.de/geschichte, accessed 23.03.2020.
Kraus, John D. 1964. Recent Advances in Radio Astronomy, IEEE Spectrum, September 1964, p. 78.
Mezger, Peter G. 1984. 50 Years of Radio Astronomy, IEEE Transactions on Microwave Theory and Techniques, Vol. MTT-32, No. 9, September 1984.
Nesti, Renzo 2019. 1933: Radio Signals from Sagittarius, IEEE Antennas & Propagation Magazine, August 2019, p. 109.
Poppe, Martin 2015. Die Maxwellsche Theorie, Wiesbaden: Springer essentials.
„radio and radar astronomy." Britannica Academic, Encyclopædia Britannica, 17 Aug. 2018, academic.eb.com/levels/collegiate/article/radio-and-radar-astronomy/62411, accessed 5. Nov. 2019.
Stephan, Karl D. 1999. How Ewen and Purcell discovered the 21-cm Interstellar Hydrogen Line, IEEE Antennas and Propagation Magazine, Vol. 41, No. 1, February 1999.

Chapter 2

https://www.swpc.noaa.gov/products/solar-cycle-progression, accessed 28.3.2020.

Chapter 3

Heuberger, Albert, Eberhard Gamm 2017. Software Defined Radio-Systeme für die Telemetrie : Aufbau und Funktionsweise von der Antenne bis zum Bit-Ausgang, Berlin, Heidelberg: Springer

Kalberla, PMW, et al. 2005: Leiden/Argentine/Bonn (LAB) survey, https://doi.org/10.1051/0004-6361:20041864.
Kark, Klaus W. 2010. Antennen und Strahlungsfelder, Wiesbaden: Vieweg+Teubner, 3. Aufl.
Welch, Peter D. 1967. The Use of Fast Fourier Transform for the Estimation of Power Spectra: A Method Based on Time Averaging Over Short, Modified Periodograms. IEEE Transactions on Audio and Electroacoustics, Vol. AU-15, No. 2, June 1967, p. 70.

Chapter 4

https://www.spaceweather.gc.ca/solarflux/sx-en.php, accessed 05.05.2020.
Ebersberger, Johannes 2020. Ein tiefer Blick in die Milchstraße, Sterne und Weltraum, Mai 2020, S. 74.
Oort, J.H. 1959. A summary and assessment of current 21-cm results concerning spiral and disk structures in our galaxy, Paris Symposium on Radio Astronomy, IAU Symposium no. 9 and URSI Symposium no. 1, held 30 July–6 August, 1958. Edited by Ronald N. Bracewell. Stanford, CA: Stanford University Press, p. 409.

Chapter 5

Ebersberger, Johannes 2017. Vom Garten in die Galaxis, Sterne und Weltraum, September 2017, S. 64.
Fritzsche, Berndt, Frank Haiduk und Uwe Knöchel 2006. Ein kompaktes Radioteleskop für Schulen, Sterne und Weltraum Dezember 2006, S. 74.
http://radioastronomie.vdsastro.de, accessed 05.05.2020.
http://www.jodrellbank.manchester.ac.uk/news-and-events/, accessed 05.05.2020.
https://astropeiler.de/, accessed 05.05.2020.
https://en.wikipedia.org/wiki/List_of_radio_telescopes, accessed 02.08.2021
https://public.nrao.edu/telescopes/vla/, accessed 05.05.2020.
https://public.nrao.edu/news/, accessed 05.05.2020.
https://vale.oso.chalmers.se/salsa/welcome, accessed 05.05.2020.
https://www.bkg.bund.de/DE/ObservatoriumWettzell/Messverfahren/Radiointerferometrie/radiointerferometrie_cont.html, accessed 05.05.2020.
https://www.camras.nl/en/, accessed 05.05.2020.
https://www.mpifr-bonn.mpg.de/pressemeldungen accessed 05.05.2020.
Leech, Marcus 2013, A 21 cm Radio Telescope for the Cost-Conscious, https://www.rtl-sdr.com/rtl-sdr-for-budget-radio-astronomy/, accessed 05.05.2020.
https://www.radio-astronomy.org, accessed 02.08.2021.
VdS-Journal für Astronomie, Nr. 71 (4/2019), Schwerpunktthema Radioastronomie.